Retrograde neurotrophin signaling through Tollo regulates synaptic growth in *Drosophila*

Shannon L. Ballard, Daniel L. Miller, and Barry Ganetzky

Laboratory of Genetics, University of Wisconsin-Madison, Madison, WI 53705

Toll-like receptors (TLRs) are best characterized for their roles in mediating dorsoventral patterning and the innate immune response. However, recent studies indicate that TLRs are also involved in regulating neuronal growth and development. Here, we demonstrate that the TLR Tollo positively regulates growth of the *Drosophila melanogaster* larval neuromuscular junction (NMJ). *Tollo* mutants exhibited NMJ undergrowth, whereas increased expression of *Tollo* led to NMJ overgrowth. *Tollo* expression in the motoneuron was both necessary and sufficient for regulating NMJ growth. Dominant genetic interactions together with altered levels of phosphorylated c-Jun N-terminal kinase (JNK) and *puc-lacZ* expression revealed that Tollo signals through the JNK pathway at the NMJ. Genetic interactions also revealed that the neurotrophin Spätzle3 (Spz3) is a likely Tollo ligand. *Spz3* expression in muscle and proteolytic activation via the Easter protease was necessary and sufficient to promote NMJ growth. These results demonstrate the existence of a novel neurotrophin signaling pathway that is required for synaptic development in *Drosophila*.

Introduction

Accurate processing of information in neural circuits requires proper development of synaptic connections between neighboring cells. Even after their establishment, synapses must maintain the ability to undergo morphological and functional modifications in response to altered activity, experience, or environment throughout an organism's life (Budnik et al., 1990; Prakash et al., 1999; Featherstone and Broadie, 2000; Packard et al., 2003; Sigrist et al., 2003; Collins and DiAntonio, 2007). Although many neurological disorders including autism, epilepsy, and neurodegeneration are associated with synaptic defects (Prakash et al., 1999; Torroja et al., 1999; Zhang et al., 2001; Johnston, 2004; Chang et al., 2008; Jeibmann and Paulus, 2009), the genetic and molecular mechanisms governing synaptic growth and plasticity remain to be fully elucidated.

The *Drosophila melanogaster* larval neuromuscular junction (NMJ) is a powerful system for dissecting mechanisms regulating synaptic growth and plasticity, and many of the known regulators are conserved with vertebrates (Keshishian et al., 1996; Featherstone and Broadie, 2000; Packard et al., 2003; Ruiz-Cañada and Budnik, 2006; Collins and DiAntonio, 2007). In both vertebrates and invertebrates, secreted growth factors and their downstream components have been implicated in regulating processes such as patterning of the nervous system, neuronal proliferation, axon guidance, neurite outgrowth, and synapse formation (Charron and Tessier-Lavigne, 2007; Mizutani and Bier, 2008; Guillemot and Zimmer, 2011; Park and Poo, 2013; Rosso and Inestrosa, 2013). Development and growth of the larval NMJ is mediated in part by growth factors such as TGF-β–bone morphogenic protein (BMP) and Wnt/Wg. The TGF-β–BMP pathway positively regulates NMJ growth in a retrograde manner, wherein the ligand (Glass bottom boat) is secreted from muscle and signals through receptors at the presynaptic terminal (McCabe et al., 2003; Marqués, 2005). The Wingless ligand, which is thought to be secreted from presynaptic terminals, signals through Frizzled2 receptors located both pre- and postsynaptically to promote NMJ growth (Packard et al., 2002; Salinas, 2005). Recently, a neuropeptide signaling pathway that exerts positive regulation of NMJ growth via the cholecystokinin-like receptor, which is localized presynaptically, and its ligand drosulfakinin, which is released by neurosecretory cells in the brain, was characterized (Chen and Ganetzky, 2012). This unexpected discovery highlights our incomplete

Correspondence to Shannon Ballard: slballard@wisc.edu

Abbreviations used in this paper: BMP, bone morphogenic protein; Brp, Bruchpilot; CNS, central nervous system; EJP, excitatory junction potential; mEJP, miniature EJP; MN, motoneuron; NF-κB, nuclear factor κB; NMJ, neuromuscular junction; pJNK, phosphorylated JNK; Spz, Spätzle; TLR, Toll-like receptor; VNC, ventral nerve cord.

The Rockefeller University Press $30.00
J. Cell Biol. Vol. 204 No. 7 1157–1172
www.jcb.org/cgi/doi/10.1083/jcb.201308115

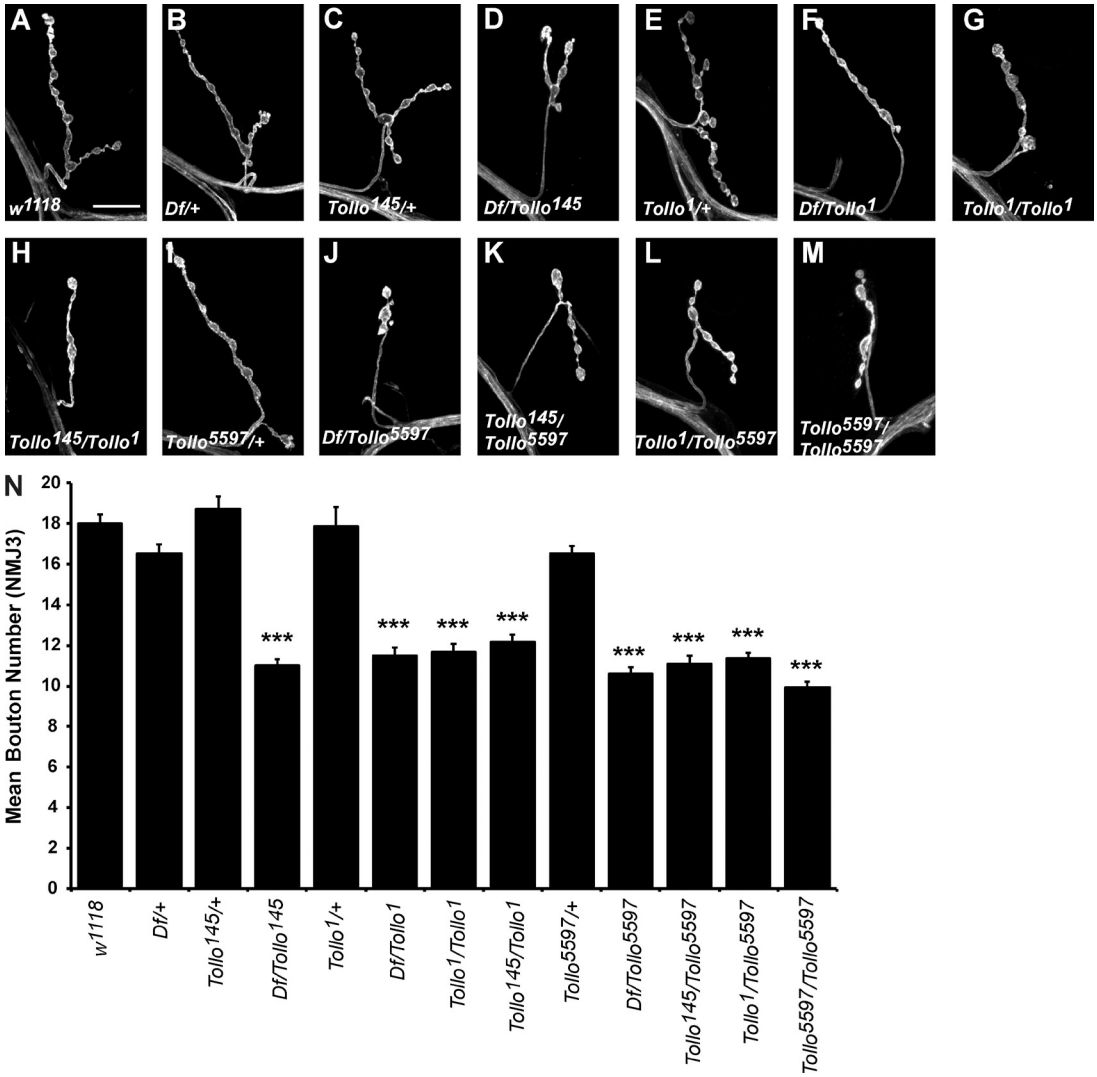

Figure 1. **Tollo promotes NMJ growth.** (A–M) Representative confocal images of NMJ3 from larvae of indicated genotypes labeled with FITC–anti-HRP. (N) Quantification of bouton numbers at NMJ3 in larvae of genotypes shown. *Tollo* mutant larvae (D, F–H, and J–M) display a significant reduction in bouton number compared with control larvae (A–C, E, and I). Error bars indicate SEM. ***, $P < 0.001$. $n \geq 19$. Bar, 20 µm.

understanding of growth factor signaling mechanisms that regulate NMJ growth and development.

Here, we show that the *Drosophila* transmembrane receptor Tollo (Toll-8), a member of the Toll-like family of receptors, is a strong positive regulator of NMJ growth. Toll-like receptors (TLRs) are type I transmembrane receptors best characterized for their roles in innate immunity and embryonic patterning (Stathopoulos and Levine, 2002; Imler and Zheng, 2004; Valanne et al., 2011). In vertebrates, TLRs are also expressed in microglia, astrocytes, oligodendrocytes, and other tissues such as epithelial cells (Imler and Zheng, 2004; Hanke and Kielian, 2011; Lee et al., 2013). TLRs can activate inflammatory pathways in response to neuronal injury, neurodegeneration, and infection. Thus, TLRs are critical mediators between the immune system and the nervous system (Tanga et al., 2005; Chen et al., 2007; Letiembre et al., 2007; Ma et al., 2007; Lee et al., 2013). Although TLRs are also expressed in neurons, their functions in neurons are only beginning to be described (Hanke and Kielian, 2011; Okun et al., 2011; Lee et al., 2013; McIlroy et al., 2013).

In *Drosophila*, Toll, the best characterized member of the TLR family, signals through nuclear factor κB (NF-κB) transcription factors (Dor and Dif) upon binding the ligand Spätzle (Spz; Anderson et al., 1985a,b; Stathopoulos and Levine, 2002; Minakhina and Steward, 2006; Ganesan et al., 2011; Valanne et al., 2011). Spz and Spz-like ligands are cysteine-knot growth factors that are similar in structure to vertebrate neurotrophins (Parker et al., 2001; Zhu et al., 2008), which are members of a key family of growth factors that regulate synaptic development and function. These secreted signaling molecules are important for stem cell survival and differentiation, axon growth and guidance, as well as synapse formation, maturation, and refinement (Chao, 2003; Park and Poo, 2013).

Recent work in *Drosophila* has shed new light on neurotrophin-like factors in invertebrates (Zhu et al., 2008). In the developing embryo, Spz2 (also called *Drosophila* Neurotrophin 1 [DNT1]) promotes cell survival in the central nervous system (CNS) and influences motor axon targeting, similar to functions of vertebrate neurotrophins (Zhu et al., 2008). In addition, embryos

mutant for *Spz5* (also called DNT2) exhibit an increase in apoptosis and a mild axon-targeting defect (Zhu et al., 2008). Six Spz-like ligands have been identified in the *Drosophila* genome (Parker et al., 2001), of which Spz2/DNT1 and Spz5/DNT2 exhibit neurotrophin-like functions in the nervous system. Here, we investigate the regulation of NMJ growth by another TLR (Tollo) and its neurotrophin family member ligand (Spz3). During preparation of this manuscript, Sutcliffe et al. (2013) reported studies on the roles of DNT1, DNT2, and Spz in NMJ growth regulation and found that these neurotrophins affect NMJ growth in a cell-specific manner: Spz regulates growth of NMJ4 whereas DNT1 and DNT2 regulate growth of NMJ6/7 (Sutcliffe et al., 2013).

We demonstrate that Tollo is required presynaptically to positively regulate NMJ growth and development. Our evidence suggests that Tollo signaling at the NMJ occurs through JNK activation of the transcription factors Jun and Fos rather than via the canonical NF-κB pathway. Genetic evidence further suggests that Spz3, secreted from the muscle, is a likely Tollo ligand. These results demonstrate that as in vertebrates a neurotrophin-like pathway in *Drosophila* plays an important role in regulating synapse growth and development at the larval NMJ.

Results

Tollo promotes NMJ growth

In the course of mapping a temperature-sensitive paralytic mutant generated in our laboratory, we tested various nearby candidate genes on chromosome arm 3L for failure of complementation. Fortuitously, we discovered that mutations of *Tollo* have an NMJ growth defect even though they complement the paralytic mutation we started with. Because of the strength of the phenotype and the inherent interest in *Tollo*, we pursued the analysis of this mutant. We found that loss-of-function mutations of *Tollo* cause a reduction in mean bouton number as well as a decrease in mean total branch length at NMJ3 (Fig. 1 and Fig. S2), without any associated reduction in muscle volume (Fig. S1). At NMJ3, the number of boutons in *Tollo* mutants is reduced by over 30% (Fig. 1 N) and the mean total branch length is shortened by at least 20% (Fig. S2) compared with wild-type or heterozygous (*Tollo*/+) controls. Although we focus on the analysis of NMJ3 in this study (see the following analysis of *Tollo* expression), we observe comparable undergrowth phenotypes for other NMJs, including NMJ4 (Fig. S2). These results identify Tollo as a positive regulator of NMJ growth.

Tollo functions presynaptically to regulate NMJ growth

To determine where *Tollo* expression is required to promote NMJ growth, we analyzed the expression pattern of a *Gal4* enhancer trap of *Tollo* by expressing a membrane-targeted GFP construct (*Tollo-Gal4>UAS-mCD8-GFP*; Fig. 2 A). This *Tollo-Gal4* recapitulates the endogenous expression pattern of *Tollo* in the imaginal wing disc (Ayyar et al., 2007). We observe strong *GFP* expression in motoneuron 3 (MN3) in wandering third instar larvae. GFP expression colocalizes with α-HRP labeling, which is specific for neuronal membranes (Fig. 2 A), indicating that *Tollo*

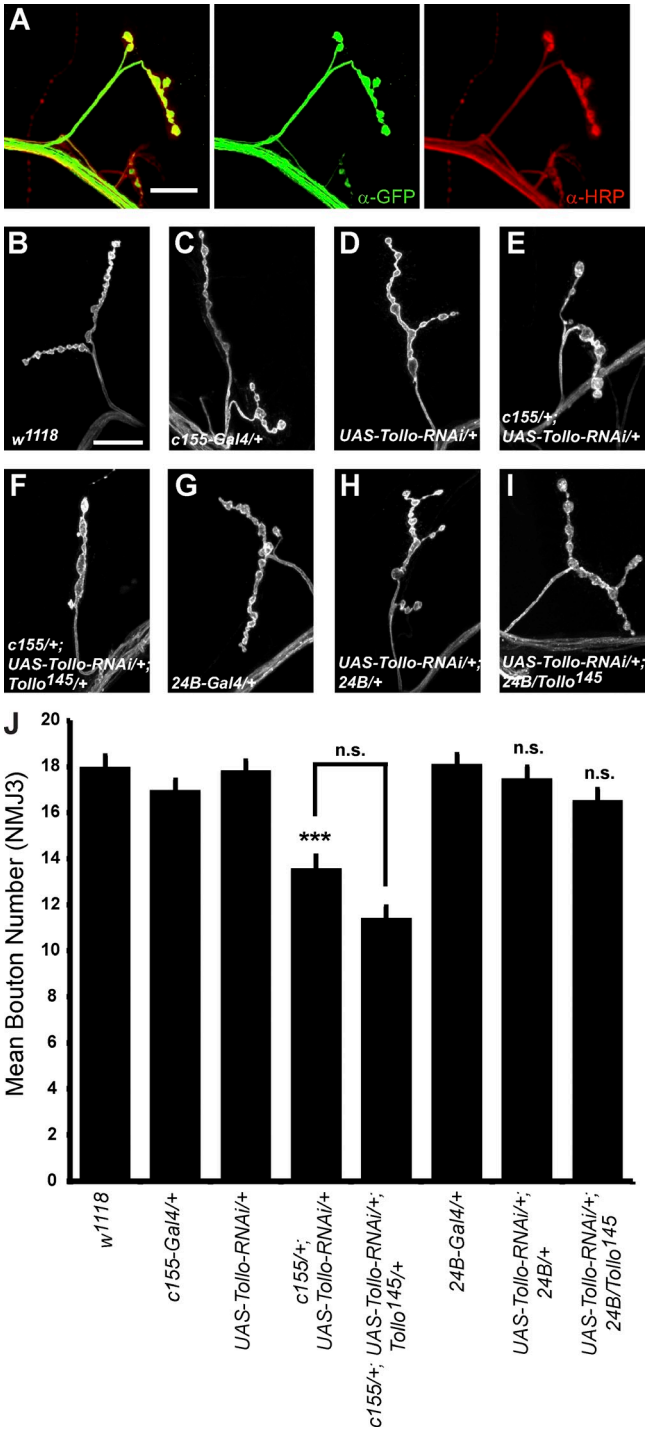

Figure 2. ***Tollo* expression is required presynaptically to promote NMJ growth.** (A) Representative confocal images of NMJ3 in *Tollo-Gal4>UAS-mCD8-GFP* larvae demonstrating that GFP is expressed presynaptically as revealed by almost complete colocalization with anti-HRP staining, which labels neuronal membranes. (B–I) Representative confocal images of NMJ3 from larvae of indicated genotypes labeled with FITC–anti-HRP. (J) Quantification of bouton numbers at NMJ3 in larvae of genotypes shown. Reduction in neuronal expression of *Tollo* (*c155/+; UAS-Tollo-RNAi/+*) leads to a decrease in bouton number (E and J) compared with control larvae (B–D and J). Further reduction in *Tollo* expression by making larvae heterozygous for *Tollo* (*c155/+; UAS-Tollo-RNAi/+; Tollo^{145}/+*) causes a larger decrease in bouton number (F and J). No significant change in bouton number is observed when *Tollo* expression is reduced in muscle (*24B/UAS-Tollo-RNAi*; G–J). Error bars indicate SEM. ***, $P < 0.001$; n.s., not statistically significant. $n \geq 24$. Bars, 20 µm.

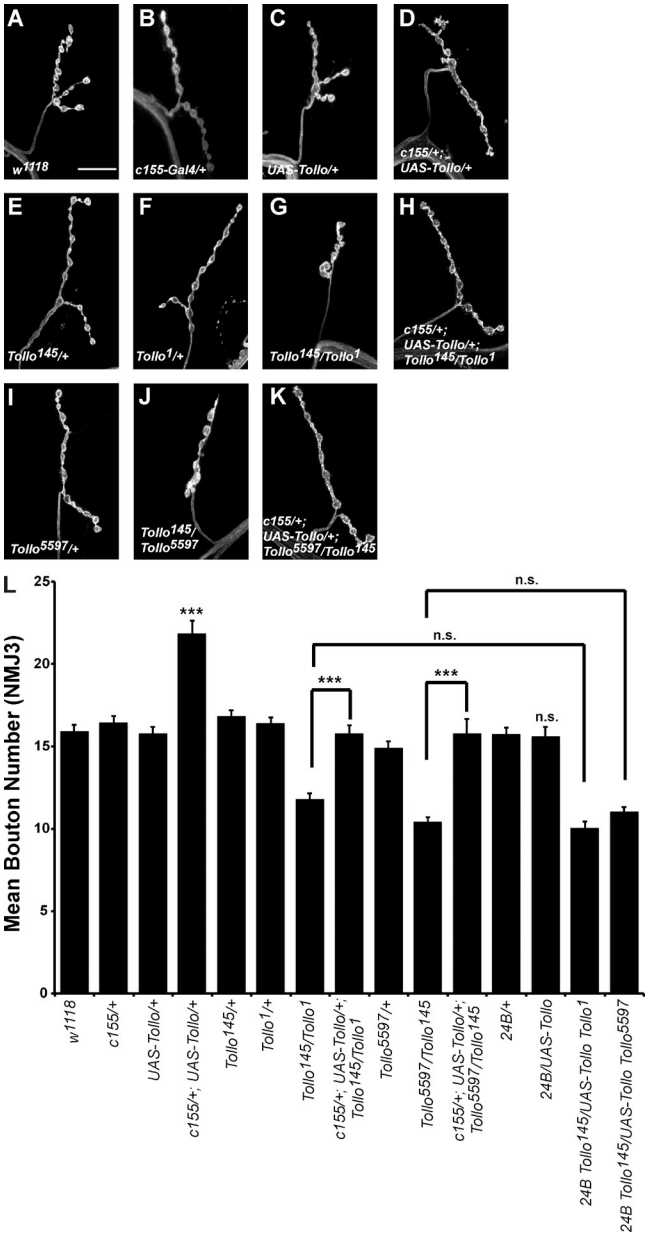

Figure 3. **Presynaptic expression of *Tollo* rescues NMJ undergrowth in *Tollo* mutants.** (A–K) Representative confocal images of NMJ3 in larvae of indicated genotypes labeled with FITC–anti-HRP. (L) Quantification of bouton numbers at NMJ3 in larvae of genotypes shown. Neuronal expression of *Tollo* in wild-type larvae (*c155/+; UAS-Tollo/+*) leads to an increase in bouton number (D and L) compared with control larvae (A–C and L). Bouton number is restored to wild-type levels in *Tollo* mutant larvae (G, J, and L) by neuronal expression of *Tollo* (e.g., *c155/+; UAS-Tollo/+; $Tollo^{5597}$/$Tollo^{145}$*; H, K, and L). Expression of *Tollo* in the muscle neither increases bouton number in wild-type larvae nor restores bouton number in *Tollo* mutant larvae (L). Error bars indicate SEM. ***, $P < 0.001$; n.s., not statistically significant. $n \geq 15$. Bar, 20 µm.

is expressed presynaptically in MNs innervating muscle 3. We also observe GFP expression in other MNs, such as those innervating muscle 4 and muscles 6/7. However, this expression was variable and weak compared with MNs that innervate more dorsally located muscles (e.g., MN3). Thus, we concentrated on the analysis of NMJ3 to investigate the role of Tollo in NMJ growth. The undergrowth phenotype in *Tollo* mutants is consistent in abdominal segments A2–A4, although the phenotype is slightly stronger in A4 compared with more anterior segments (Fig. S2).

To test whether *Tollo* is required presynaptically to regulate NMJ growth, we reduced *Tollo* expression using the neuronal-specific elav^{c155}-*Gal4* driver and RNAi directed against *Tollo* transcripts. We observe a significant decrease in bouton number in *c155>UAS-Tollo-RNAi* larvae compared with controls (Fig. 2, B–E and J). Moreover, *c155>UAS-Tollo-RNAi* larvae heterozygous for a *Tollo* mutation (*c155/+; UAS-Tollo-RNAi/+; $Tollo^{145}$/+*) display a further reduction in bouton number (Fig. 2, F and J). In contrast, we did not observe any significant reduction in bouton number when *Tollo* mRNA is reduced postsynaptically using the muscle-specific *24B-Gal4* even when *Tollo* expression was further reduced by heterozygosity for a *Tollo* mutation (Fig. 2, B, D, and G–J).

Conversely, presynaptic expression of *Tollo* in an otherwise wild-type larva (*c155>UAS-Tollo*) leads to a significant increase in bouton number compared with control larvae (Fig. 3, A–D and L), whereas, postsynaptic expression of *Tollo* (*24B>UAS-Tollo*) does not affect bouton number (Fig. 3 L). Moreover, *c155>UAS-Tollo* expression in *Tollo* mutants fully rescues bouton number to wild-type levels (Fig. 3, E–L). However, *24B>UAS-Tollo* expression does not alter bouton number in *Tollo* mutants (Fig. 3 L). Together, these data demonstrate that *Tollo* expression in neurons is necessary and sufficient to promote NMJ growth.

Tollo is not required for normal synaptic function

Because Tollo function is required in MNs for normal NMJ growth during development, loss of *Tollo* could also result in altered synaptic function at the NMJ. Thus, we examined the amplitude of evoked excitatory junction potentials (EJPs) and spontaneous miniature EJPs (mEJPs) at muscle 3 in *Tollo* mutant larvae. At 1 and 0.4 mM Ca^{2+}, EJP amplitude is normal (Fig. 4, G–K; and Fig. S3). At 1 mM Ca^{2+}, the frequency and amplitude of mEJPs as well as quantal content of evoked neurotransmitter release were all normal in *Tollo* mutant larvae (Fig. 4, A–F and L). These data indicate that despite the reduction in bouton number in *Tollo* mutants, basic aspects of synaptic transmission at the NMJ are unimpaired. We also examined synaptic structure at a finer level in *Tollo* mutants and found no differences from controls in the apposition of presynaptic (Bruchpilot [Brp]) and postsynaptic (GluRIII) components of active zones (Kittel et al., 2006; Wagh et al., 2006) or in the ratio of GluRIIA/GluRIIB levels in postsynaptic receptor fields (Marrus et al., 2004; Fig. S4).

Because synaptic function and organization are normal in *Tollo* mutants, whereas bouton number is decreased, one possible compensatory mechanism would be an increase in the number of active zones in each bouton. To examine this possibility, we quantified the mean number of BRP puncta in *Tollo* mutants. Compared with control larvae, *Tollo* mutants display an increase in the mean number of BRP puncta per bouton (Fig. 5, A–E). In contrast, the volume of boutons in *Tollo* mutants does not differ from controls (Fig. S1). Thus, the density of BRP puncta is increased in *Tollo* mutant boutons relative to controls (Fig. 5 G).

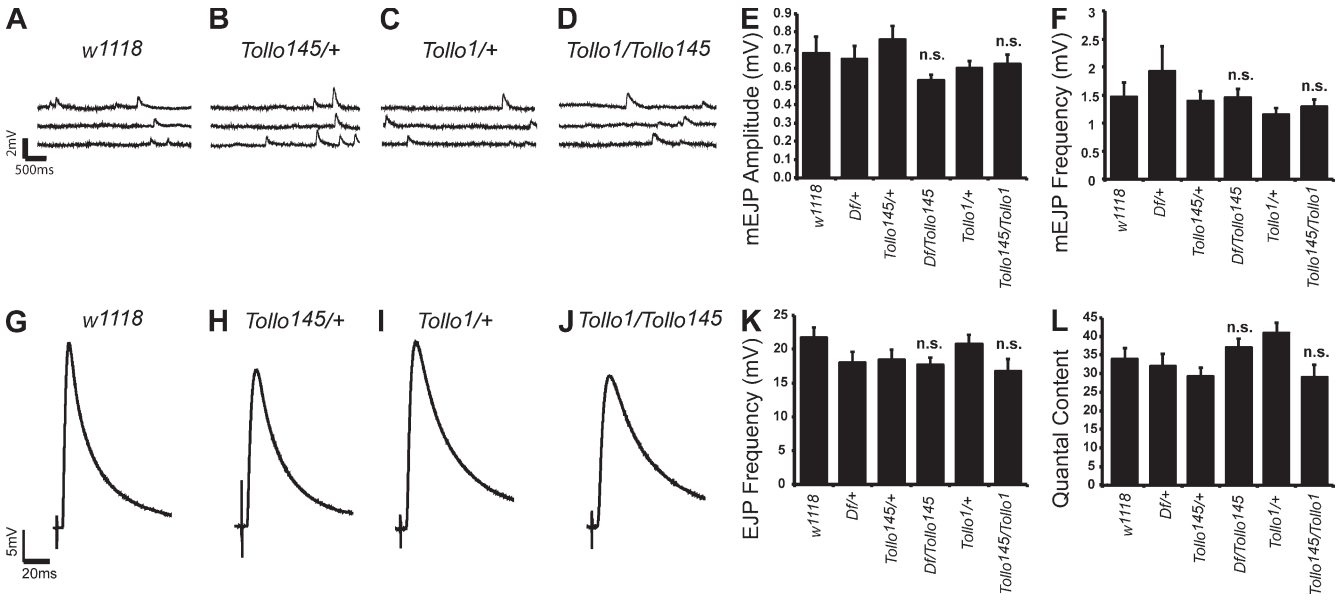

Figure 4. **Synaptic function is not altered in *Tollo* mutant larvae.** (A–D) Representative traces of spontaneous neurotransmitter release recorded in 1.0 mM Ca^{2+} from muscle 3 of indicated genotypes. (E and F) Quantification of the mean mEJP amplitude (E) and frequency (F) from muscle 3 of indicated genotypes. (G–J) Representative traces of evoked transmitter release recorded in 1.0 mM Ca^{2+} from muscle 3 of indicated genotypes. (K) Quantification of the mean EJP amplitude from muscle 3 in third instar larvae of indicated genotypes. Neither mean EJP amplitude, mEJP frequency, nor mEJP amplitude are affected in *Tollo* mutant larvae compared with controls. (L) Quantal content is unaffected in *Tollo* mutant larvae compared with controls. $n \geq 13$. Error bars indicate SEM. n.s., not statistically significant.

The proportionate increase in active zones per bouton in *Tollo* mutants is almost the same as the proportionate reduction in bouton number per NMJ. Thus, despite NMJ undergrowth in *Tollo* mutants, the total number of active zones per NMJ remains close to normal (Fig. 5 F).

Tollo signals through the JNK pathway to regulate NMJ growth

In both *Drosophila* and vertebrates, Toll and TLRs signal through highly conserved downstream components (Belvin and Anderson, 1996; O'Neill and Greene, 1998; Imler and Zheng, 2004). Receptor activation leads to activation of the interleukin-1 receptor-associated kinase, which, in turn, leads to phosphorylation and degradation of inhibitor κB (Cactus in *Drosophila*). Loss of inhibitor κB relieves cytoplasmic sequestration of the transcription factor NF-κB (Dorsal in *Drosophila*). NF-κB then enters the nucleus to regulate transcription of target genes (Belvin and Anderson, 1996; O'Neill and Greene, 1998; Imler and Zheng, 2004). To examine whether Tollo signals through this canonical pathway, we tested whether there were any dose-dependent dominant interactions between *Tollo* and *dorsal* mutations. We observed no change in bouton number in larvae doubly heterozygous for *Tollo* and *dorsal* (i.e., *Tollo* +/+ *Dorsal*; Fig. S5). If Cactus functions in MNs to inhibit growth-promoting functions of Tollo signaling, we would expect to observe a decrease in bouton number when *cactus* is overexpressed with *c155-Gal4*. However, overexpression of *cactus* in neurons had no effect on bouton number (Fig. S5). Moreover, Dorsal and Cactus are localized postsynaptically in muscle and regulate postsynaptic glutamate receptor localization via a nontranscriptional mechanism (Cantera et al., 1999; Heckscher et al., 2007), whereas, as described earlier, we do not observe any alteration in glutamate receptor levels or localization in *Tollo* mutants (Fig. S4). These data suggest that Tollo is not signaling through the canonical Toll pathway at the NMJ.

In response to immune and stress signals, vertebrate Toll/Interleukin-1 receptors can signal through noncanonical pathways such as a MAPK cascade (O'Neill and Greene, 1998; Ruse and Knaus, 2006; Chen et al., 2007). To investigate whether Tollo regulates NMJ growth through a MAPK pathway, we examined bouton number in larvae heterozygous for mutations of both *Tollo* and *basket* (*bsk*), which encodes a JNK that is activated by MAPK-dependent phosphorylation. Whereas *bsk*/+ or *Tollo*/+ heterozygotes alone do not affect NMJ growth, *bsk*/+*; Tollo*/+ double heterozygotes exhibit a significant decrease in bouton number (Fig. 6, A–H and Q). This dominant genetic interaction between *Tollo* and *bsk* suggests that Tollo is signaling through a JNK pathway to regulate NMJ growth.

The idea that Tollo signals through a JNK pathway predicts a decrease in levels of phosphorylated JNK (pJNK) in *Tollo* mutants. To examine this prediction, we used an antibody specific for the phosphorylated form of JNK to analyze levels of pJNK at NMJs in *Tollo* mutant larvae. Contrary to the study by Seppo et al. (2003) but consistent with the findings of Yagi et al. (2010), we did not observe any decrement in HRP levels at NMJs in *Tollo* mutants compared with control larvae (Fig. S1). Consequently, to quantify pJNK levels we measured the fluorescence intensity ratio of anti-pJNK to anti-HRP (see Materials and methods) in *Tollo* mutants and control larvae (Fig. 7, A–E). *Tollo* mutant NMJs exhibit a significant decrease in normalized pJNK fluorescence intensity as expected if Tollo signals through a JNK pathway. Moreover, the fact that we observe a decrease in pJNK levels in synaptic boutons suggests that Tollo may function locally in presynaptic terminals to initiate a positive NMJ growth signal, although we cannot rule out the possibility that some Tollo signaling

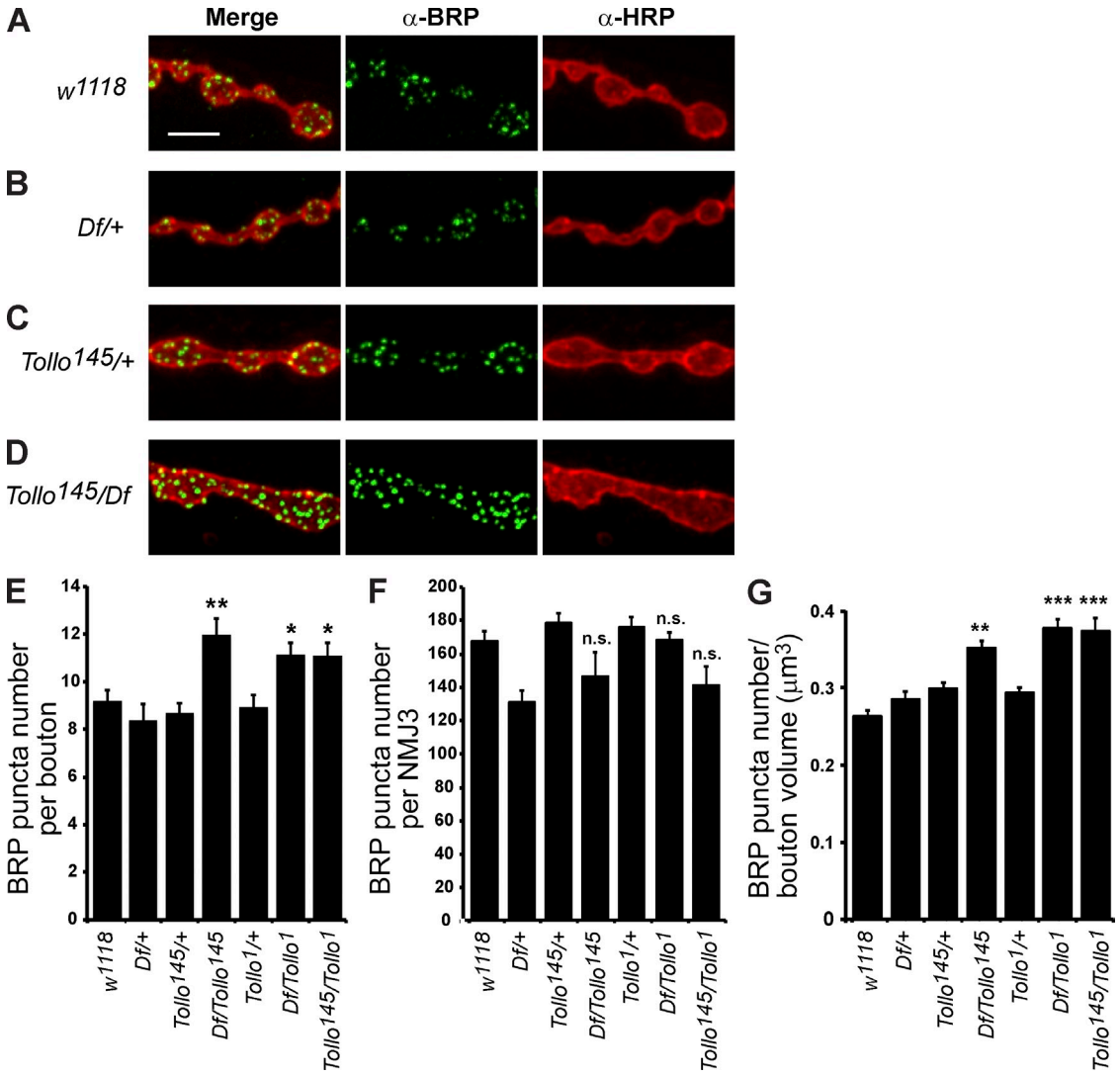

Figure 5. **BRP puncta number is altered in boutons of *Tollo* mutants.** (A–D) Representative confocal images of NMJ3 of indicated genotypes labeled with anti-BRP (green) and Cy3–anti-HRP (red). (E) Quantification of BRP puncta per bouton at NMJ3 for larvae of indicated genotypes. (F) Quantification of total BRP puncta per NMJ3 for larvae of indicated genotypes. $n \geq 10$. (G) Density of BRP puncta in individual boutons for larvae of indicated genotypes. *Tollo* mutant larvae display an increase in the number and density of BRP puncta per bouton (D, E, and G) relative to control larvae (A–C, E, and G). However, total number of BRP puncta per NMJ is not affected in *Tollo* mutants compared with control larvae (F). Error bars indicate SEM. *, $P < 0.05$; **, $P < 0.01$; ***, $P < 0.001$; n.s., not statistically significant. $n \geq 89$. Bar, 5 µm.

occurs back in the MN cell body. In either case, the positive growth signal ultimately is likely to require transcriptional activation of target genes in the nucleus.

If Tollo signaling activates the JNK pathway, we predict that an increase in *Tollo* expression should increase JNK activity. To test this, we used the *puc-lacZ* reporter, an enhancer trap of the JNK phosphatase encoded by *puckered* (*puc*), whose expression is activated by JNK (Martín-Blanco et al., 1998). We examined expression of *puc-lacZ* in *Tollo-Gal4* expressing cells in the ventral region of the abdominal ventral nerve cord (VNC) where MN3 cell bodies are located (Landgraf et al., 1997). In control larvae, *puc-lacZ* expression levels are low (Fig. 7, F and I), and it is detected in relatively few *Tollo-Gal4* expressing cells (Fig. 7, F and H). When *Tollo* is overexpressed using the *Tollo-Gal4* driver (*Tollo-Gal4>UAS-Tollo*), we observe an increase in the number of *puc-lacZ* expressing nuclei (Fig. 7, G and H) as well as an increase in *puc-lacZ* fluorescence intensity in those cells expressing *Tollo-Gal4* (Fig 7, G and I). Together, the decrease in presynaptic levels of pJNK in *Tollo* mutants and the increase in *puc-lacZ* expression when *Tollo* is overexpressed, strongly support the conclusion that Tollo activates the JNK signaling cascade in MNs.

Tollo genetically interacts with the Jun and Fos transcription factors

The major downstream effectors of the JNK pathway are the transcription factors Jun and Fos, which function both individually and as a heterodimeric (AP1) complex to regulate expression of various target genes. Both Jun and Fos have previously been implicated in regulating NMJ growth and plasticity (Sanyal et al., 2002, 2003; Collins et al., 2006). Thus, one or both of these transcription factors are likely candidates for mediating

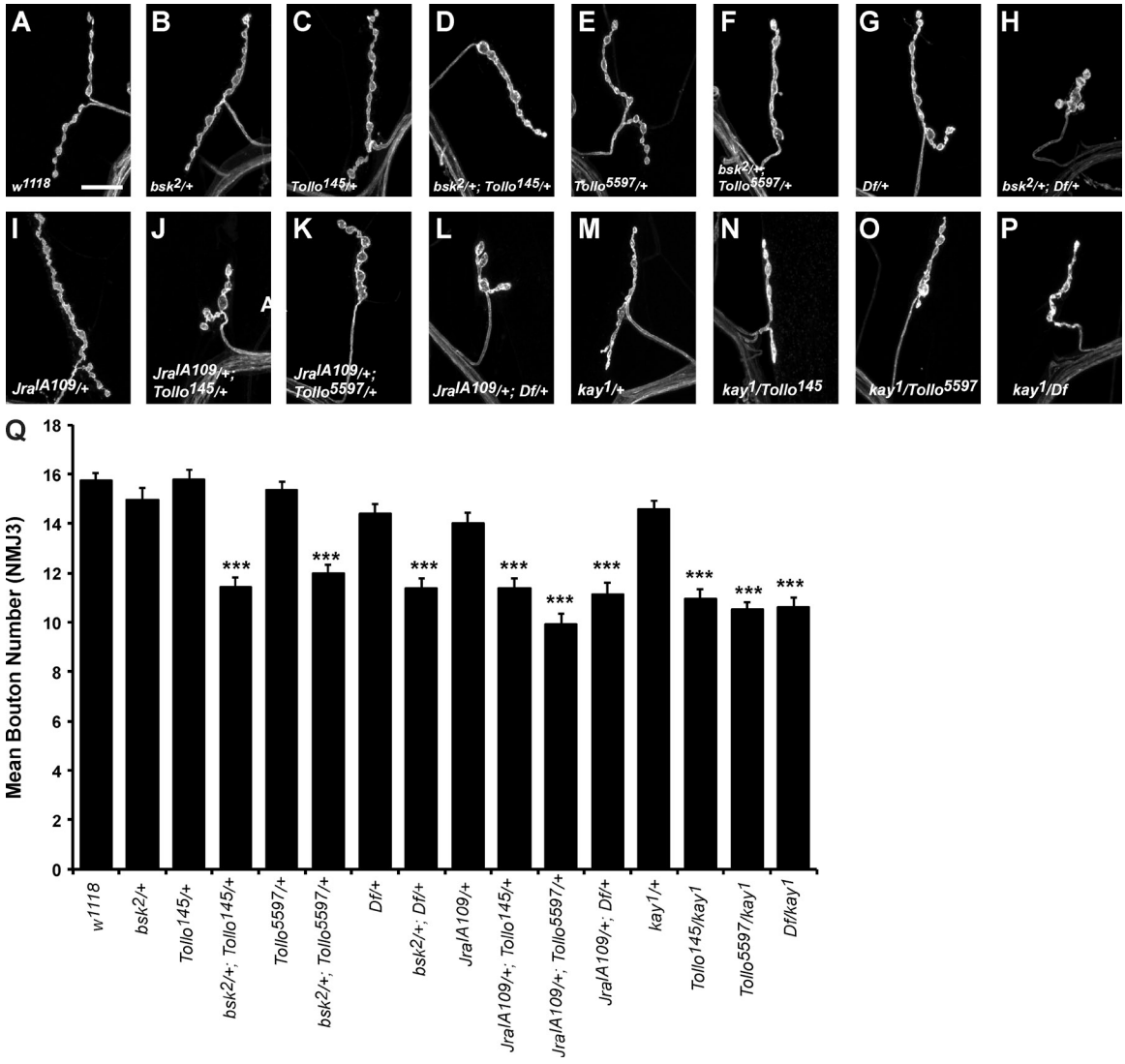

Figure 6. ***Tollo* interacts genetically with components of the JNK pathway to promote NMJ growth.** (A–P) Representative confocal images of NMJ3 in larvae of indicated genotypes labeled with FITC–anti-HRP. (Q) Quantification of bouton numbers at NMJ3 in larvae of genotypes shown. Larvae heterozygous for both *Tollo* and *bsk* (D, F, and Q), *Tollo* and *Jra (=DJun;* J, K, and Q), or *Tollo* and *kay (=DFos;* N, O, and Q) or hemizygous for *Tollo* and heterozygous for *bsk*, *Jra*, or *kay* (H, L, P, and Q) display a reduction in bouton number at NMJ3 compared with control larvae (A–C, E, G, I, M, and Q). Error bars indicate SEM. ***, $P < 0.001$. $n \geq 30$. Bar, 20 µm.

the effect of Tollo signaling on NMJ growth. We again used a genetic approach to examine this possibility by testing whether *Tollo* also exhibits dominant interactions in combination with mutations of Jun (encoded by *Jra*) and Fos (encoded by *kayak*; Fig. 6). Larvae doubly heterozygous for both *Tollo* and *Jra* mutations (*Jra/+; Tollo/+)* display a significant decrease in bouton number (Fig. 6, A–J and P). We observe a comparable dominant interaction between *Tollo* and *kayak* (Fig. 6, K–P). These results support the conclusion that Tollo positively regulates NMJ growth by stimulating Jun and Fos activity via activation of JNK.

Tollo signaling is likely activated by the putative neurotrophin Spz3

To identify other components of the Tollo signaling pathway, we screened deletions to uncover genes that interact with *Tollo* in a dose-dependent manner to reduce bouton number in *Df/+; Tollo/+* larvae. From this screen, we discovered that deletions or mutations of *Spz3* dominantly interact with *Tollo* (Fig. 8). We then tested deletions that uncover several other Spz family genes for similar dominant interactions with *Tollo*. Only a few of the family members exhibit a dominant interaction with *Tollo*, of which *Spz3* and *Spz5* exhibit the most robust interactions. We subsequently focused on the analysis of *Spz3* because it exhibited the strongest dominant interaction with *Tollo*. Larvae hemizygous for *Spz3* and heterozygous for *Tollo* (i.e., *Spz3-Df/+; $Tollo^{145}$/+*) display a significant reduction in bouton number compared with controls (Fig. 8, A–F and U). We observe a comparable but somewhat weaker interaction in *$Spz3^{P}$/+; $Tollo^{145}$/+* larvae, where *$Spz3^{P}$* is a hypomorphic P-element insertional allele of *Spz3* (Fig. 8, G, I, J, and U). Larvae mutant for *Spz3* (*Spz3-Df/$Spz3^{P}$*) also display a reduction in bouton number compared with controls (Fig. 8, A, B, G, H, and U). Moreover, in larvae hemizygous for a *Tollo* mutation or carrying a heteroallelic combination of *Tollo* mutations, the decrease in bouton

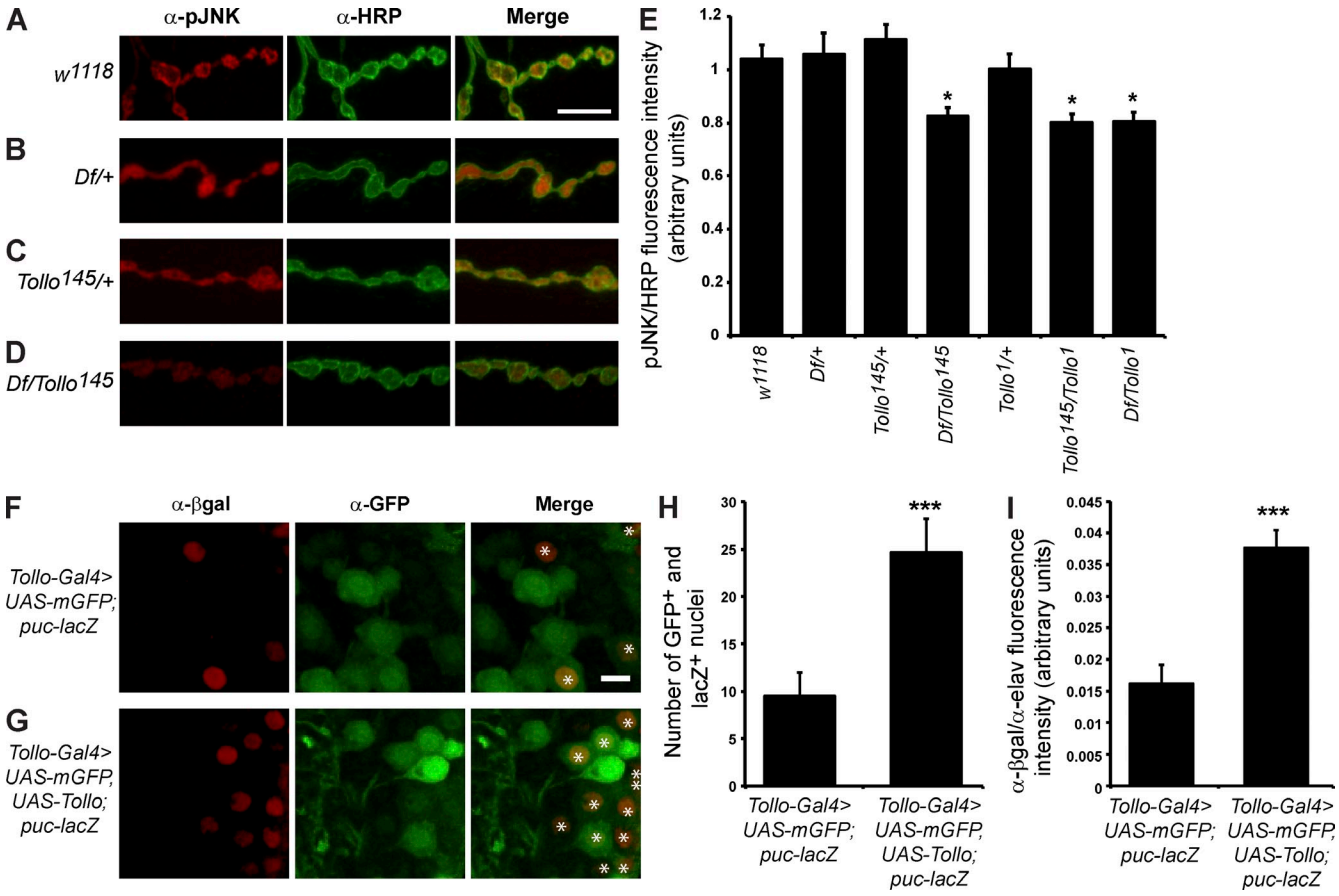

Figure 7. ***Tollo* signals through the JNK pathway.** (A–D) Representative confocal images of boutons at NMJ3 in larvae of genotypes shown labeled with anti-pJNK (left) and FITC–anti-HRP (middle). (E) Quantification of the pJNK/HRP fluorescence intensity ratio for individual boutons at NMJ3. *Tollo* mutant larvae exhibit a decrease in pJNK/HRP fluorescence levels (D and E) compared with control larvae (A–C and E). $n = 10$. (F and G) Representative confocal images of regions of the ventral half of the larval abdominal VNC labeled with anti-βgal (left) and anti-GFP (middle). Cells labeled with both antibodies (e.g., those expressing both *puc-lacZ* and *mCD8-GFP*) are marked with asterisks in merged images. (H) Quantification of number of nuclei expressing both *puc-lacZ* and *Tollo-Gal4*-driven mGFP in the ventral half of the abdominal VNC in larvae of indicated genotypes. (I) Quantification of puc-lacZ:elav fluorescence intensity ratio for ventral half of abdominal VNC in larvae of indicated genotypes. Increased expression of *Tollo* in *Tollo-Gal4* expressing cells causes an increase in the number of cells that express *puc-lacZ* and in the level of *puc-lacZ* expression. $n = 6$. Error bars indicate SEM. *, $P < 0.05$; ***, $P < 0.001$. Bars: (A–D) 10 µm; (F and G) 5 µm.

number (Fig. 8, K, M, and U) is further enhanced by a partial reduction of *Spz3* levels (*Spz3^{P}/+; Tollo^{145}/Tollo^{5597}*; Fig. 8, L, N, and U). Conversely, the NMJ overgrowth associated with presynaptic expression of *Tollo* (*c155/+; UAS-Tollo/+*; Fig. 3 and Fig. 8, O and U) is suppressed back to wild-type levels by partial reduction of *Spz3* (e.g., *c155/+; UAS-Tollo/Spz3^{P}*; Fig. 3 and Fig. 8, O–Q and U). These results demonstrate that Spz3 is a positive regulator of NMJ growth and most likely functions as a ligand that activates the Tollo receptor. Consistent with this idea, we found that *Spz3-Df/Spz3^{P}* larvae display a significant reduction in pJNK levels compared with control larvae (Fig. 9), as expected if Spz3 signals through Tollo to promote the phosphorylation of JNK.

During embryonic patterning, Spz is cleaved by Easter, a serine protease, to generate an active Toll ligand (DeLotto and DeLotto, 1998). Thus, it was of interest to determine whether *easter* (*ea*) also plays a role in regulating NMJ growth. We observe that *ea^{1} +/+ Tollo^{145}* larvae exhibit NMJ undergrowth comparable to that of *Spz3^{P}/+; Tollo^{145}/+* larvae (Fig. 8, S and U). NMJs in larvae doubly heterozygous for *Spz3* and *ea* (*Spz3^{P}/+; ea^{1}/+*) are similarly undergrown (Fig. 8, T and U). Thus, Easter is required for normal NMJ growth, presumably by cleavage and activation of the Spz3 ligand.

Spz3 expression is required postsynaptically to regulate NMJ growth

If Spz3 is a Tollo ligand that promotes NMJ growth, what is the source of this signal? To address this question, we examined the effect of tissue-specific reduction in *Spz3* expression on NMJ growth. Using the pan-neuronal *c155-Gal4* driver to express *UAS-Spz3-RNAi* (*c155>UAS-Spz3-RNAi*), we do not observe any effect on NMJ growth (Fig. 10, A–D and R). Moreover, neuronal-specific reduction of *Spz3* does not affect NMJ growth even in a sensitized *Tollo/+* background (*c155/+; UAS-Spz3-RNAi/+; Tollo^{145}/+*; Fig. 10, E, F, and R). In contrast, when the *24B-Gal4* driver was used to reduce *Spz3* expression in muscle (*24B-Gal4>UAS-Spz3-RNAi*), we observe a significant decrease in bouton number (Fig. 10, A, C, G, H, and R). We observe a comparable decrease in NMJ growth when *easter* expression is reduced in muscle (*24B-Gal4>UAS-ea-RNAi*; Fig. 10, P–R). Moreover,

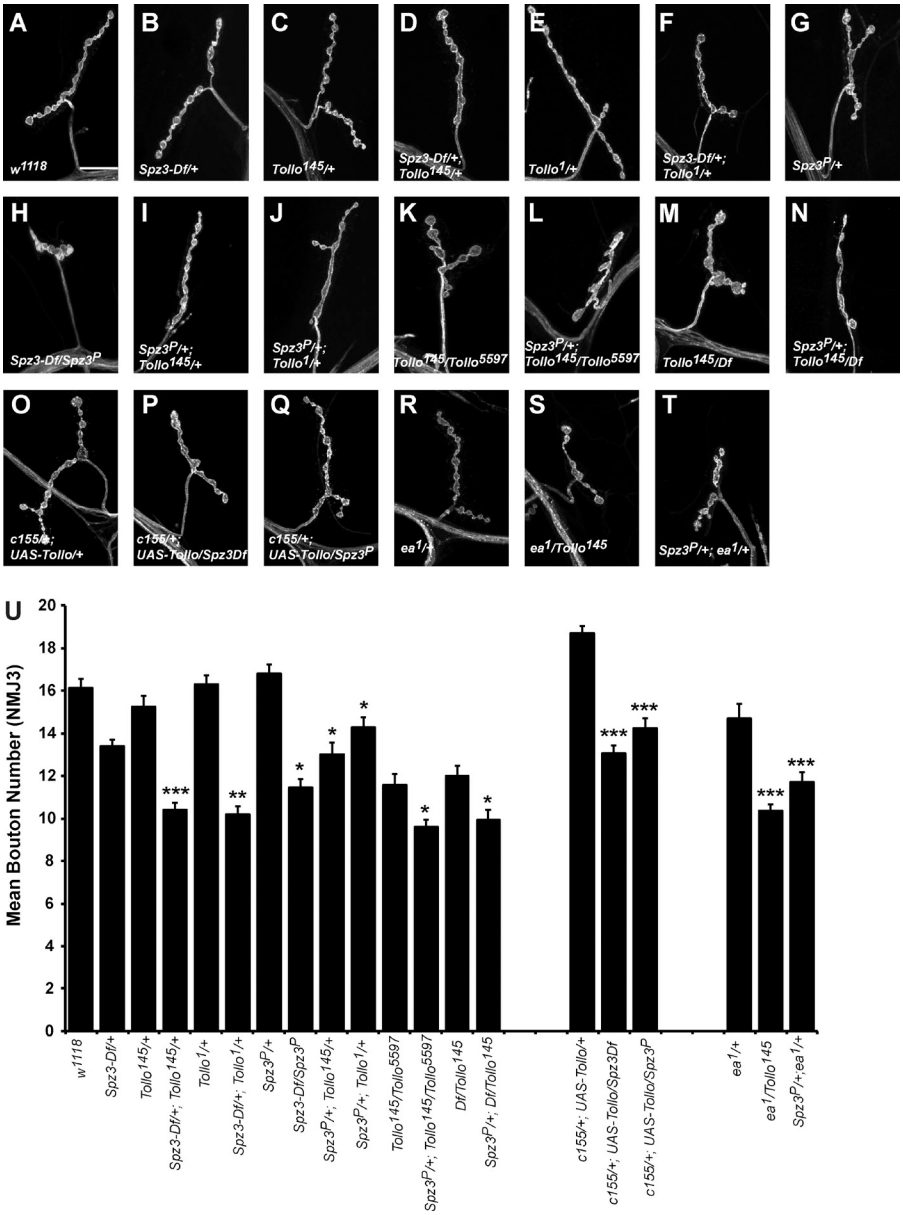

Figure 8. ***Tollo* interacts genetically with *Spz3* and *easter* to promote NMJ growth.** (A–T) Representative confocal images of NMJ3 in larvae of indicated genotypes labeled with FITC–anti-HRP. (U) Quantification of bouton numbers at NMJ3 in larvae of genotypes shown. Larvae heterozygous for *Tollo* and hemizygous for *Spz3* (D, F, and U) or heterozygous for both *Tollo* and *Spz3* (I, J, and U) exhibit a decrease in bouton number compared with control larvae (A–C, E, G, and U). *Spz3* mutant larvae display a reduction in bouton number (H and U) compared with control larvae (A, B, G, and U). Homozygous *Tollo* mutant larvae (K, M, and U) display a further reduction in bouton number when heterozygous for *Spz3* (L and N). A reduction in *Spz3* (P, Q, and U) suppresses the NMJ overgrowth observed in *c155/+; UAS-Tollo/+* larvae (O and U). Larvae heterozygous for *ea* and *Tollo* (S and U) or *Spz3* (T and U) show a decrease in bouton number compared with control larvae (A, C, G, R, and U). Error bars indicate SEM. *, $P < 0.05$; **, $P < 0.01$; ***, $P < 0.001$. $n \geq 11$. Bar, 20 µm.

bouton number is further reduced in *24B-Gal4>UAS-Spz3-RNAi* larvae that are hemizygous for *Spz3* (*24B-Gal4>UAS-Spz3-RNAi/Spz3-Df*) or heterozygous for *Tollo* (*UAS-Spz3-RNAi/+; 24B-Gal4/Tollo*^{145}; Fig. 10, J, K, and R).

To further examine the spatial requirement for *Spz3* expression, we assessed the phenotypic effects on NMJ growth when *Spz3* was overexpressed in different tissues in an otherwise wild-type background. Consistent with our aforementioned results, pan-neuronal expression of *Spz3* (*c155-Gal4>UAS-Spz3*) has no effect on NMJ growth (Fig. 10, M and R), whereas expression in muscle (*24B-Gal4>UAS-Spz3*) enhances NMJ growth (Fig. 10, N and R). This increase in NMJ growth is mediated through the Tollo pathway because it is fully suppressed by heterozygosity for *Tollo* (Fig. 10, O and R). Together, these data demonstrate that Spz3, produced and potentially cleaved in muscle, is sufficient to promote NMJ growth by activation of the Tollo receptor at the presynaptic terminal.

Discussion

Using a phenotype-based approach, we discovered a novel signaling pathway mediated by the TLR, Tollo, and its presumptive ligand Spz3, a neurotrophin-like molecule that positively regulates NMJ growth in *Drosophila* larvae via activation of a JNK cascade. These studies define new roles both for TLRs and neurotrophin-like ligands in the regulation of synaptic growth in *Drosophila*.

Role of TLRs in nervous system development

TLRs are highly conserved between *Drosophila* and vertebrates (Imler and Zheng, 2004). Toll was first identified in *Drosophila* for its role in dorsoventral patterning in the embryo (Anderson et al., 1985a,b). Subsequent studies revealed that TLRs also play a key role in regulating the innate immune response in

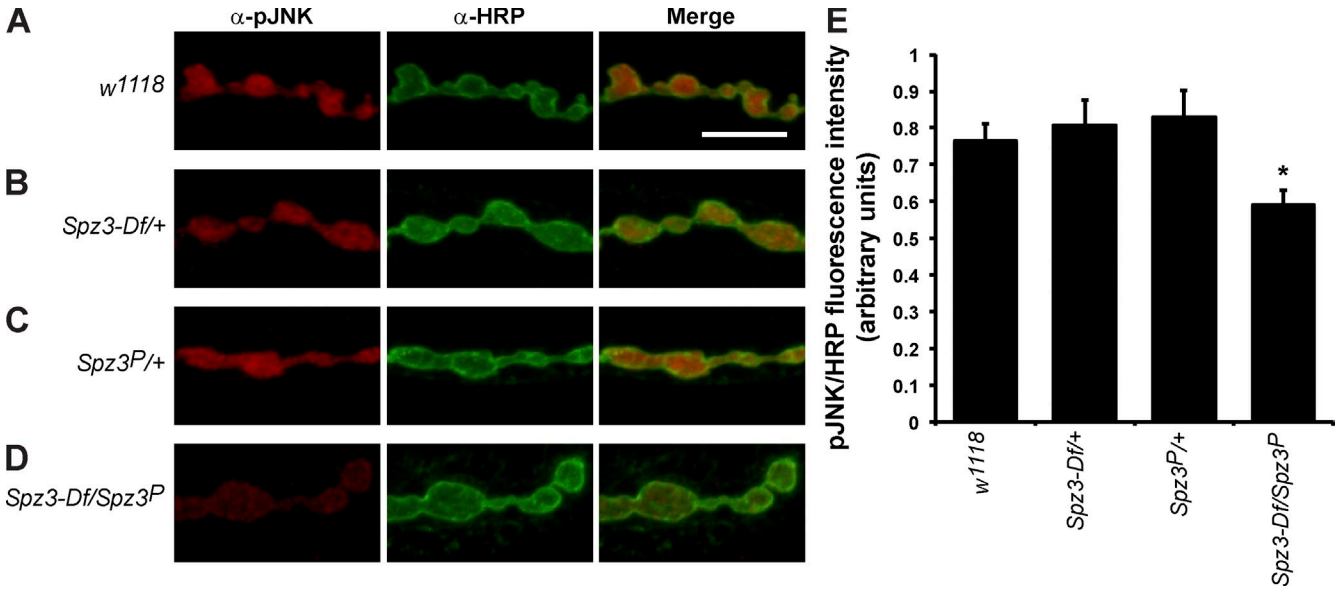

Figure 9. **Spz3 influences the levels of pJNK at the NMJ.** (A–D) Representative confocal images of boutons at NMJ3 in larvae of genotypes shown labeled with anti-pJNK (left) and FITC–anti-HRP (middle). (E) Quantification of the pJNK/HRP fluorescence intensity ratio for individual boutons at NMJ3. *Spz3* mutant larvae exhibit a decrease in pJNK/HRP fluorescence levels (D and E) compared with control larvae (A–C and E). Error bars indicate SEM. *, $P < 0.05$. $n = 10$. Bar, 10 µm.

both *Drosophila* and vertebrates (Takeda et al., 2003; Imler and Zheng, 2004; Valanne et al., 2011). Discovery of TLR expression in specific cell types in the vertebrate nervous system, including astrocytes, oligodendrocytes, and microglia, has implicated TLRs in neural plasticity, neural progenitor cell proliferation and differentiation, neurite outgrowth, neuroprotection, and learning and memory (Hanke and Kielian, 2011; Okun et al., 2011; Hanamsagar et al., 2012). Although TLRs are also expressed in vertebrate neurons, the functional consequences of this expression and pathways through which neuronal TLRs function have not been fully elucidated. A recent study in *Drosophila* revealed that Toll-6 and Toll-7 are expressed in the *Drosophila* CNS and are required for development of the nervous system, including proper targeting of MNs in embryos (McIlroy et al., 2013).

We have found that Tollo function is required in *Drosophila* larval MNs to promote NMJ growth. Together with similar findings reported by McIlroy et al. (2013), this study reveals a new role for TLR signaling in the nervous system.

Tollo signals through the JNK pathway to promote NMJ growth

RNAi expression, transgenic rescue, and expression analysis of a *Tollo-Gal4* enhancer trap line demonstrate that Tollo functions presynaptically in MNs to promote NMJ growth, consistent with a previous study demonstrating that *Tollo* is expressed during formation of neural lineages (Brody et al., 2002). In addition, FlyAtlas analysis (Chintapalli et al., 2007) reveals that *Tollo* is expressed at high levels in the larval CNS. Recent studies have shown that other *Drosophila* TLRs are also expressed in the nervous system (McIlroy et al., 2013). Thus, it is very likely that *Tollo* expression is required within MNs to regulate NMJ growth.

In other developmental contexts in *Drosophila* and vertebrates, canonical Toll signaling is mediated by activation of NF-κB transcription factors (Dorsal and Dif in *Drosophila*) via degradation of inhibitor κB (Cactus in *Drosophila*; Stathopoulos and Levine, 2002; Minakhina and Steward, 2006). However, for larval NMJ phenotypes, we do not observe any dominant genetic interactions in double mutant combinations of *Tollo* with *dorsal*, and overexpression of *cactus* in the MN does not affect NMJ growth. These results are consistent with previous findings that *dorsal* and *cactus* are expressed postsynaptically in muscle (Cantera et al., 1999) to regulate localization of glutamate receptors (Heckscher et al., 2007). In contrast, we do observe dominant phenotypic interactions of *Tollo* in combination with components of the JNK signaling pathway, including JNK (*basket*), Jun (*Jra*), and Fos (*kayak*). These results strongly suggest that Tollo signals presynaptically through a downstream JNK pathway to positively regulate NMJ growth. Consistent with this idea, we find that pJNK is reduced in boutons in *Tollo* mutants and expression of the puc-lacZ reporter is increased when *Tollo* is overexpressed. Although we have not confirmed that total levels of JNK in boutons remain unchanged in *Tollo* mutants because of technical difficulties associated with ubiquitous expression of JNK in other cell types such as muscle and glia, all of our results support the conclusion that Tollo is signaling through the JNK pathway to regulate NMJ growth. The most parsimonious hypothesis is that signaling through Tollo receptors occurs locally at motor terminals, but in the absence of a Tollo antibody, we cannot rule out the possibility that some Tollo receptors are localized at the MN cell body. In any case, execution of the Tollo-dependent growth signal likely requires transcriptional activation of target genes back in the nucleus.

Jun and Fos, the two components of the AP1 transcription factor complex, are expressed in larval MNs and known to be involved in regulating NMJ growth (Sanyal et al., 2002, 2003). Neuronal expression of dominant-negative forms of Fos or Jun causes NMJ undergrowth whereas overexpression of AP1 leads to an increase in bouton number (Sanyal et al., 2002, 2003). Fos

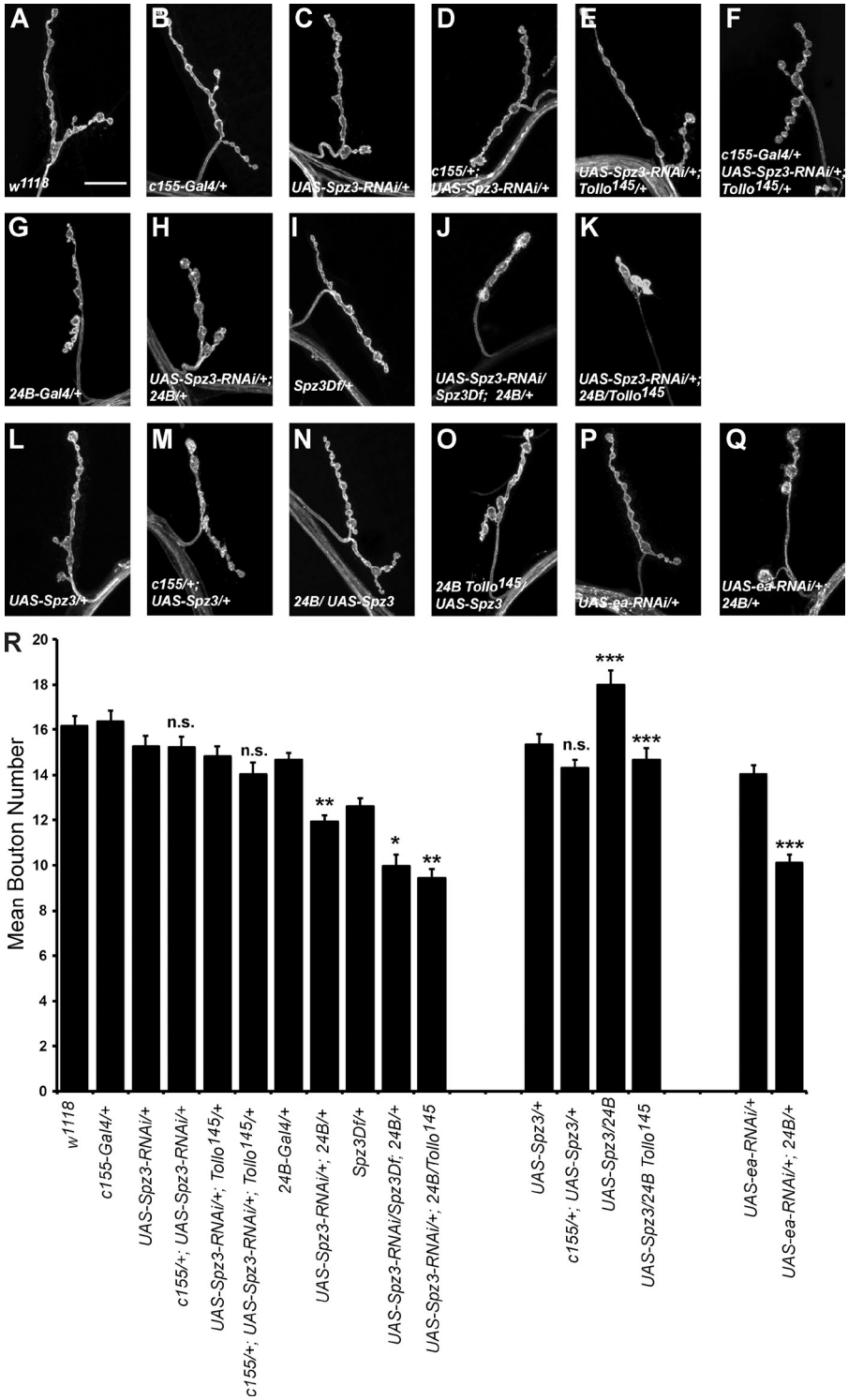

Figure 10. **Postsynaptic expression and activation of *Spz3* is required to promote NMJ growth.** (A–Q) Representative confocal images of NMJ3 in larvae of indicated genotypes labeled with FITC–anti-HRP. (R) Quantification of bouton numbers at NMJ3 in larvae of genotypes shown. Neuronal reduction of *Spz3* transcripts either in an otherwise wild-type background (D) or in a heterozygous *Tollo* mutant background (F) does not cause a reduction in bouton number compared with controls (A–C and R). In contrast, reduction of *Spz3* expression in muscle (H and R) leads to a decrease in bouton number compared with control larvae (A, C, G, and R). Bouton number is further decreased when muscle expression of *Spz3* is reduced in a background hemizygous for *Spz3* (J and R) or heterozygous for a *Tollo* mutation (K and R). Neuronal overexpression of *Spz3* does not affect bouton number (M and R). However, overexpression of *Spz3* in muscle (N and R) results in an increase in bouton number compared with control larvae (A, G, L, and R). This overgrowth is suppressed to wild-type levels when larvae are heterozygous for *Tollo* (O and R). Reduction of *ea* expression in muscle leads to a decrease in bouton number (Q and R) relative to control larvae (A, G, and P). Error bars indicate SEM. *, $P < 0.05$; **, $P < 0.01$; ***, $P < 0.001$; n.s., not statistically significant. $n \geq 26$. Bar, 20 µm.

and Jun share common functions as components of AP1, but they also have distinct functions in certain cells and tissues at particular developmental stages (Riesgo-Escovar and Hafen, 1997). For example, mutations of *hiw* (*highwire*) cause striking NMJ overgrowth via Wnd (Wallenda), a MAPKKK protein, which in turn regulates NMJ growth through Fos but not Jun (Collins et al., 2006). Thus, Jun and Fos can function separately in the regulation of NMJ growth. The dominant genetic interactions we observe in heterozygous double mutant combinations of *Tollo* with either *Jun* or *Fos* suggest that Tollo can signal through both components of AP1, but whether Jun and Fos are acting individually to regulate NMJ growth or jointly as the AP1 complex remains to be determined.

Tollo does not impair synaptic transmission

Despite a 30% reduction in bouton number at NMJ3 in *Tollo* mutant larvae, the basic parameters of synaptic function, such as mEJP size and frequency and quantal content, remain normal.

This uncoupling between NMJ size and function has been observed in many other instances. For example, *hiw* mutations cause a very striking increase in bouton number, but synaptic transmission is reduced. Moreover, *wnd* mutations suppress NMJ overgrowth in *hiw* but not the defect in synaptic transmission (Collins et al., 2006). Thus, there is no direct correlation between morphology and function, presumably because Hiw acts on different downstream targets in the regulation of these two processes.

The lack of correlation between bouton number and synaptic strength is readily explained by Peled and Isacoff (2011), who demonstrate that most presynaptic active zones have a very low release probability. At each NMJ, there are only a small number of high probability release sites and these tend to be located at distal boutons (Peled and Isacoff, 2011). Thus, because overall synaptic transmission relies on relatively few active zones, synaptic function in *Tollo* mutants may not be affected if the number of high probability release sites remains normal. In addition, some type of homeostatic mechanism may act to compensate for the decrease in bouton number in *Tollo* mutants based on our observation that the number of active zones per bouton is increased compared with controls. The net result is that the total number of active zones per NMJ is not altered in *Tollo* mutants. A previous study has shown that glutamate receptors preferentially cluster opposite larger and more active sites (Marrus and DiAntonio, 2004). As another compensatory mechanism to maintain synaptic function, it may be possible that active zones are larger in *Tollo* mutants and thus have greater synaptic strength.

The absence of a defect in synaptic function in our experiments contrasts with a previous study showing that AP1 expression at the NMJ affects synaptic strength: simultaneous overexpression of *Fos* and *Jun* produced an increase in EJC amplitude whereas overexpression of either *Fos* or *Jun* alone had no effect (Sanyal et al., 2002). Moreover, overexpression of dominant-negative forms of *Jun* or *Fos* caused a decrease in EJC amplitude. Because *Tollo* genetically interacts with both *Jun* and *Fos* in regulating NMJ growth, a decrease in synaptic transmission might have been predicted based on these previous studies (Sanyal et al., 2002, 2003). One possible explanation is that overexpression of either wild-type or dominant-negative *Jun* and *Fos* transgenes is likely to have stronger consequences on AP1 function than partial or complete loss of *Tollo* because Jun and Fos are thought to be downstream of multiple signaling pathways at the NMJ, including pathways with greater effects on both bouton number and electrophysiology. Moreover, the situation may be further complicated by the possibility that Jun and Fos are activated via distinct signaling pathways to regulate NMJ growth and function. Thus, Tollo could be required to activate Jun and Fos for NMJ growth whereas some other pathways are required to activate these proteins to regulate NMJ function.

Spz3, a neurotrophin-like ligand, signals through Tollo at the NMJ

In an unbiased screen for genes that interact with *Tollo* at the NMJ, we found that *Spz3* genetically interacts with *Tollo* to promote NMJ growth. Similar to *Tollo* mutants, *Spz3* mutants display a decrease in bouton number, indicating that Spz3 positively regulates NMJ growth. Our genetic analyses strongly suggest that Spz3 is expressed in abdominal muscles and is a ligand for the Tollo receptor at the NMJ. First, *Spz3* and *Tollo* interact in a dominant, dose-dependent manner to cause NMJ undergrowth. Second, a partial reduction in *Spz3* levels suppresses NMJ overgrowth associated with overexpression of *Tollo* in MNs. Third, RNAi knockdown of *Spz3* in muscles causes NMJ undergrowth that becomes enhanced in a heterozygous *Tollo* mutant background. Fourth, heterozygosity for a *Tollo* mutation completely suppresses the NMJ overgrowth associated with overexpression of *Spz3* in muscles. This interpretation is consistent with a recently published parallel study showing that other Spz-like ligands are expressed in larval abdominal muscles (Sutcliffe et al., 2013) and with FlyAtlas (Chintapalli et al., 2007) data indicating high levels of *Spz3* expression in larval carcasses, which are enriched for abdominal muscles. Together, these genetic data imply that Spz3 functions through the Tollo receptor to promote NMJ growth, but direct biochemical evidence of Spz3 as the Tollo ligand awaits confirmation.

Tollo genetically interacts with components of the JNK pathway to promote NMJ growth, and loss of *Tollo* leads to a decrease in the levels of pJNK at the NMJ. Because our data indicate that Spz3 signals through Tollo at the NMJ, we examined the levels of pJNK at the NMJ and found a significant decrease in *Spz3* mutant larvae relative to controls. Thus, the data suggest a signaling pathway at the NMJ whereby Spz3 activates the Tollo receptor, which then activates the JNK signaling cascade.

The identification of Spz3 as a likely Tollo ligand is of particular interest because Spz and the Spz-like ligands are cysteine knot growth factors proposed to be *Drosophila* neurotrophins based on their structural homology with vertebrate neurotrophins (in particular brain-derived neurotrophic factor; DeLotto and DeLotto, 1998; Parker et al., 2001; Zhu et al., 2008). In the developing *Drosophila* embryo, Spz2 (renamed DNT1) functions similarly to vertebrate neurotrophins by promoting cell survival in the CNS and affecting motor axon targeting (Zhu et al., 2008). Mutations in *Spz5* (DNT2) influence neuronal survival with modest effects on axon targeting (Zhu et al., 2008). In addition to our findings with Spz3, Sutcliffe et al. (2013) recently found that Spz, DNT1, and DNT2 also regulate NMJ growth in a cell-specific manner. Thus, Spz affects NMJ4, whereas DNT1 and DNT2 affect NMJ6/7. Although the precise effect on NMJ growth varies with different Spz/DNT ligands and specific motor terminal affected, our studies together with those of Sutcliffe et al. (2013) demonstrate that Spz-like ligands play important and previously unrecognized roles in regulating NMJ development.

Since their discovery in vertebrates, numerous studies have characterized the role of these growth factors in multiple different aspects of neuronal survival, growth, function, and plasticity (Chao, 2003; Park and Poo, 2013). However, only recently have neurotrophin-like proteins been found in invertebrates, and their identification as bona fide neurotrophins still engenders some controversy. A neurotrophin-like protein (ApNT) whose structural and functional properties are conserved with vertebrate neurotrophins was recently reported in *Aplysia* (Kassabov et al., 2013). Importantly, this study also identified a conserved Trk receptor (ApTrk) through which ApNT functions to regulate neurite

outgrowth and long-term facilitation (Kassabov et al., 2013). Vertebrate neurotrophins signal either through Trk or p75 receptors, and identification of a corresponding receptor in *Aplysia* strongly argues that ApNT is a true invertebrate neurotrophin. Conversely, Kassabov et al. (2013) question the identity of Spz and Spz-like ligands as bona fide neurotrophins, emphasizing the fact that an orthologous neurotrophin receptor has not been identified in *Drosophila*. In this context, it is of interest that the ligand binding domain of TLRs is similar to that of the ligand binding domain of Trk receptors (Bothwell, 2006). In addition, Toll and $p75^{NTR}$ activate NF-κB signaling through interleukin-1 receptor-associated kinase, MyD88, and TRAF proteins (O'Neill and Greene, 1998; Zapata et al., 2000; Mamidipudi et al., 2002; Bothwell, 2006; Valanne et al., 2011), and vertebrate $p75^{NTR}$ can bind *Drosophila* TRAF1 (Zapata et al., 2000). Similar to our findings with Tollo at the larval NMJ, the vertebrate $p75^{NTR}$ can also signal through the JNK cascade (Roux and Barker, 2002; Chao, 2003). Thus, the identity of Spz3 and other family members as true *Drosophila* neurotrophins cannot be readily dismissed.

In any case, our study convincingly demonstrates that Spz3, a protein with neurotrophin-like features, functions in a neurotrophic-like manner to promote NMJ growth. We have focused on the interaction between *Spz3* and *Tollo*. However, we note that our data do not exclude the possibility that other Spz-like ligands can signal through Tollo or that Spz3 can signal through other TLRs at the NMJ. Similar to vertebrate neurotrophins, Spz and its relatives including Spz3 require proteolytic cleavage for activation (DeLotto and DeLotto, 1998; Park and Poo, 2013). Spz is cleaved in the developing embryo by the secreted serine protease, Easter. Genetic interactions between *ea* and *Spz3* as well as between *ea* and *Tollo* suggest that Spz3 is also cleaved and activated by Easter in muscles during NMJ growth regulation.

In summary, we have uncovered a novel retrograde signaling pathway that promotes growth of the larval NMJ. We propose that Spz3, a neurotrophin-like ligand, is secreted by muscle and activates presynaptic Tollo receptors thereby triggering a downstream JNK cascade that culminates in activation of Jun and Fos and transcription of their target genes that ultimately dictate NMJ growth. This study provides important new information about regulation of NMJ development and also defines a novel role for Tollo receptors in synaptic development. It will be of interest to determine how this retrograde signaling pathway is integrated with other signaling pathways, such as BMP signaling, which also acts in a retrograde manner to stimulate NMJ growth.

Materials and methods

Fly stocks

w^{1118} was used as a wild-type control for genetic background. $Tollo^{145}$, which is an imprecise P-element excision that removes the genomic sequence −1,560 to −351 bp upstream of the translational start site, and $Tollo^{5597}$, where P{lacW} is inserted 439 bp upstream of the translational start site (Kim et al., 2006), were provided by J. Yim (Seoul National University, Seoul, Korea). $Tollo^{1}$, which is an imprecise P-element excision that removes 2,247 bp including part of the *Tollo* gene and the translational start site, and *Tollo-Gal4*, which is a Gal4 enhancer trap of *Tollo* (Ayyar et al., 2007), were provided by P. Simpson (University of Cambridge, Cambridge, UK). $cact^{D13}$ (Govind et al., 1993), which is a hypomorphic allele of *cactus* generated by EMS mutagenesis, and *UAS-cactus* (Qiu et al., 1998) were provided by S. Govind (The City College of New York, New York, NY). *puc-lacZ*^{E69} (Martín-Blanco et al., 1998), which is a *lacZ* enhancer trap of *puc*, was provided by D. Bohmann (University of Rochester, Rochester, NY). The following fly lines were obtained from the Bloomington Stock Center: *Df(3L)BSC578* (Tollo deficiency), *Df(2L)BSC234* (Spz3 deficiency), $Spz3^{EY06670}$ ($Spz3^{P}$), bsk^{2}, Jra^{IA109}, kay^{1}, ea^{1}, elav^{c155}-*Gal4*, *24B-Gal4*, and dl^{4}. The following RNAi lines were obtained from the Vienna *Drosophila* RNAi Center: *UAS-Tollo-RNAi* (13549), *UAS-Spz3-RNAi* (18949), and *UAS-ea-RNAi* (102357). For a complete list of all genotypes examined in this study and their bouton counts, see Table S1. All crosses were performed on cornmeal/molasses fly medium and maintained at 25°C.

Immunohistochemistry

Female larvae were dissected in Ca^{2+}-free saline and fixed in 4% paraformaldehyde for 18–20 min or in cold methanol for 5 min (GluR antibodies). Larval body walls were incubated in primary and secondary antibodies overnight at 4°C. Body wall preparations were mounted in VectaShield (Vector Laboratories) for microscopic analysis. Larval brains were placed on poly-lysine–coated coverslips, dehydrated through ethanol series, cleared in xylenes, and then mounted in DPX (Sigma-Aldrich). The following antibodies were used: FITC- or Cy3-conjugated anti-HRP (Jackson ImmunoResearch Laboratories, Inc.) at 1:100, Texas red–X Phalloidin (Life Technologies) at 1:1,000, rabbit or chicken anti-GFP (Invitrogen) at 1:1,000, rabbit anti-pJNK (Cell Signaling Technology) at 1:1,000, rabbit anti-βgal (MP Biomedicals) at 1:1,000, rat anti-elav (Developmental Studies Hybridoma Bank) at 1:100, mouse anti-nc82 (Brp; Developmental Studies Hybridoma Bank) at 1:250, mouse anti-GluRIIA at 1:100 (Developmental Studies Hybridoma Bank), rabbit anti-GluRIIB (raised against ASSAKKKKKTRRIEK in Marrus et al. [2004]) at 1:2,500, and rabbit anti-GluRIII (raised against QGSGSSSGSNNAGRGEKEARV in Marrus et al. [2004]) at 1:1,000 (A. DiAntonio, Washington University, St. Louis, MO). Species-specific Alexa 488, 568, or 647 secondary antibodies were used at 1:500 (Invitrogen).

Imaging and quantification

Quantification of bouton number was performed at NMJ3 because of the expression pattern of *Tollo-Gal4* (Ayyar et al., 2007) and its relative simplicity. However, comparable phenotypes were observed at other NMJs where *Tollo-Gal4* is expressed. Segments A2–A4 were analyzed for bouton number and branch length. For quantification, we defined a bouton as a discrete synaptic swelling labeled with the presynaptic marker α-HRP. The muscle size was similar in all larvae examined. At least 10 NMJs of each genotype were analyzed, and all genotypes were examined simultaneously for each experiment. Confocal images were obtained at 21–23°C on a confocal microscope (LSM 510; Carl Zeiss) with a Plan Apochromat 63× NA 1.4 oil differential interference contrast objective and accompanying software. Images were processed in ImageJ (National Institutes of Health) and Photoshop (Adobe) software. Branch length was determined using ImageJ, where arbors of primary and secondary branches were measured starting at the first bouton or branch point after defasiculation (whichever occurred first). pJNK and *puc-lacZ* fluorescence intensity was measured using methods described previously (Mosca and Schwarz, 2010a,b). For pJNK analysis, confocal z stacks of distal and proximal boutons were imported into ImageJ and converted into multichannel composite images. A region of interest was drawn around the terminal bouton as well as an internal bouton based on the HRP fluorescence channel. The mean fluorescence intensity was determined for the HRP channel and the pJNK channel. For *puc-lacZ* analysis, 2 µm of confocal slices of the ventral region of the abdominal VNC were imported into ImageJ and converted into multichannel composite images. A region of interest was taken of abdominal segments that contained *puc-lacZ*–positive nuclei that also expressed *Tollo-Gal4*. The mean fluorescence intensity was determined for the anti-elav channel and anti-βgal channel. All samples were processed under the same conditions and imaged using the same confocal parameters. The ratio of pJNK to HRP or puc-lacZ to Elav fluorescence was then determined. The fluorescence intensity for an internal and a terminal bouton were measured for 10 NMJs or for six abdominal ganglia. To determine muscle or bouton volume, confocal stacks were imported into Amira software (Visualization Sciences Group). Muscles from segment A3 (n = 10) or individual boutons ($n \geq 89$) were reconstructed by selecting and assigning pixels throughout the series of images in the confocal stack. Muscle or bouton volume was measured using the approximate voxel dimensions (in micrometers).

Molecular cloning

UAS-Tollo comprises the full-length *Tollo* sequence cloned into pUAST-attB. cDNA constructs were generated by amplification of the *Tollo* coding sequence from a full insert cDNA clone (Berkeley *Drosophila* Genome Project LD33590). UAS-Spz3 comprises a full-length *Spz3* sequence cloned into

pUAST-attB. cDNA constructs were generated by amplification of the *Spz3* sequence from a full insert cDNA clone (Berkeley *Drosophila* Genome Project RE22741). After germline transformation, *UAS-Tollo* and *UAS-Spz3* were inserted into attP40 and attP2, respectively, in a w^{1118} background. To facilitate directional cloning into pUAST-attB, primers were created with unique restriction sites that flank the open reading frames. The sequences of primers used are provided in Table S2. All constructs were sequenced for accuracy.

Electrophysiology

Electrophysiology was performed on muscle 3 in segments A2–A5 of wandering third instar larvae using standard techniques (Jan and Jan, 1976). Dissections were performed in HL3.1 saline containing 0.0 mM Ca^{2+}, and intracellular recordings were performed in HL3.1 containing the indicated Ca^{2+} concentration (Feng et al., 2004). Recording electrodes (resistance: 15–20 MΩ) were filled with 3M KCl and stimulating electrodes with saline. Recordings were acquired using pClamp10 software (Molecular Devices). Mean EJP amplitudes were calculated from 40 consecutive traces (20–60 of 60 stimulations). Mean mEJP amplitude and frequency were determined using Mini Analysis Software (v. 6.0.7; Synaptosoft). Quantal content was determined by dividing the mean EJP amplitude of a synapse by the mean mEJP amplitude from the same synapse. For this calculation, EJP amplitudes were corrected for nonlinear summation according to McLachlan and Martin (1981).

Statistical analyses

Error bars represent SEM. We performed one-way analysis of variance followed by post-hoc tests with Tukey-Kramer correction for multiple comparisons. We report the significance values to be <0.05, 0.01, or 0.001 denoted by one, two, or three asterisks, respectively.

Online supplemental material

Fig. S1 shows that muscle volume, bouton volume, and HRP levels are unaltered in *Tollo* mutants. Fig. S2 shows that branch length at NMJ3, bouton number at NMJ4, and bouton number at NMJ3 in segments in abdominal segment A2, A3, or A4 are significantly reduced in *Tollo* mutants compared with control larvae. Fig. S3 shows that synaptic function is not altered in *Tollo* mutants at NMJ3 in 0.4 mM Ca^{2+}. Fig. S4 shows that the apposition of pre- and postsynaptic components and the levels of GluRIIA and GluRIIB are unaltered in *Tollo* mutants. Fig. S5 shows that *Tollo* does not dominantly interact with components of the canonical Toll pathway, *dorsal* and *cactus*, at the NMJ and that neuronal expression of *cactus*, which is a negative regulator of the canonical Toll pathway, does not influence NMJ growth. Table S1 presents quantification of bouton number (±SEM) for each genotype presented in this manuscript along with the number of NMJs analyzed for each genotype. Table S2 presents sequences of primers used in the generation of constructs used. Online supplemental material is available at http://www.jcb.org/cgi/content/full/jcb.201308115/DC1.

We are grateful to J. Yim, P. Simpson, D. Bohmann, A. DiAntonio, the Bloomington Stock Center, and the Vienna *Drosophila* RNAi Center for providing fly stocks and antibodies. Anti-Brp, anti-GluRIIA, and anti-elav were obtained from the Developmental Studies Hybridoma Bank developed under the auspices of the National Institutes of Health, National Institute of Child Health and Human Development, and maintained by the Department of Biology at The University of Iowa. We thank Julie Simpson and Stefan Pulver for help with electrophysiology, Lingling Ho for help with DNA injection, Troy Shirangi and members of the Ganetzky laboratory for helpful discussion and comments on the manuscript, and Kathryn Narem and Ashley Arthur for technical assistance.

This research was supported by National Institutes of Health grants R01NS15390 (B. Ganetzky) and F32NS067843 (S.L. Ballard).

The authors declare no competing financial interests.

Submitted: 20 August 2013
Accepted: 12 February 2014

References

Anderson, K.V., L. Bokla, and C. Nüsslein-Volhard. 1985a. Establishment of dorsal-ventral polarity in the *Drosophila* embryo: the induction of polarity by the Toll gene product. *Cell*. 42:791–798. http://dx.doi.org/10.1016/0092-8674(85)90275-2

Anderson, K.V., G. Jürgens, and C. Nüsslein-Volhard. 1985b. Establishment of dorsal-ventral polarity in the *Drosophila* embryo: genetic studies on the role of the Toll gene product. *Cell*. 42:779–789. http://dx.doi.org/10.1016/0092-8674(85)90274-0

Ayyar, S., D. Pistillo, M. Calleja, A. Brookfield, K. Gittins, C. Goldstone, and P. Simpson. 2007. NF-κB/Rel-mediated regulation of the neural fate in *Drosophila*. *PLoS ONE*. 2:e1178. http://dx.doi.org/10.1371/journal.pone.0001178

Belvin, M.P., and K.V. Anderson. 1996. A conserved signaling pathway: the *Drosophila* toll-dorsal pathway. *Annu. Rev. Cell Dev. Biol.* 12:393–416. http://dx.doi.org/10.1146/annurev.cellbio.12.1.393

Bothwell, M. 2006. Evolution of the neurotrophin signaling system in invertebrates. *Brain Behav. Evol.* 68:124–132. http://dx.doi.org/10.1159/000094082

Brody, T., C. Stivers, J. Nagle, and W.F. Odenwald. 2002. Identification of novel *Drosophila* neural precursor genes using a differential embryonic head cDNA screen. *Mech. Dev.* 113:41–59. http://dx.doi.org/10.1016/S0925-4773(02)00010-2

Budnik, V., Y. Zhong, and C.F. Wu. 1990. Morphological plasticity of motor axons in *Drosophila* mutants with altered excitability. *J. Neurosci.* 10:3754–3768.

Cantera, R., T. Kozlova, C. Barillas-Mury, and F.C. Kafatos. 1999. Muscle structure and innervation are affected by loss of Dorsal in the fruit fly, *Drosophila melanogaster*. *Mol. Cell. Neurosci.* 13:131–141. http://dx.doi.org/10.1006/mcne.1999.0739

Chang, H.C., D.N. Dimlich, T. Yokokura, A. Mukherjee, M.W. Kankel, A. Sen, V. Sridhar, T.A. Fulga, A.C. Hart, D. Van Vactor, and S. Artavanis-Tsakonas. 2008. Modeling spinal muscular atrophy in *Drosophila*. *PLoS ONE*. 3:e3209. http://dx.doi.org/10.1371/journal.pone.0003209

Chao, M.V. 2003. Neurotrophins and their receptors: a convergence point for many signalling pathways. *Nat. Rev. Neurosci.* 4:299–309. http://dx.doi.org/10.1038/nrn1078

Charron, F., and M. Tessier-Lavigne. 2007. The Hedgehog, TGF-β/BMP and Wnt families of morphogens in axon guidance. *Adv. Exp. Med. Biol.* 621:116–133. http://dx.doi.org/10.1007/978-0-387-76715-4_9

Chen, K., J. Huang, W. Gong, P. Iribarren, N.M. Dunlop, and J.M. Wang. 2007. Toll-like receptors in inflammation, infection and cancer. *Int. Immunopharmacol.* 7:1271–1285. http://dx.doi.org/10.1016/j.intimp.2007.05.016

Chen, X., and B. Ganetzky. 2012. A neuropeptide signaling pathway regulates synaptic growth in *Drosophila*. *J. Cell Biol.* 196:529–543. http://dx.doi.org/10.1083/jcb.201109044

Chintapalli, V.R., J. Wang, and J.A. Dow. 2007. Using FlyAtlas to identify better *Drosophila melanogaster* models of human disease. *Nat. Genet.* 39:715–720. http://dx.doi.org/10.1038/ng2049

Collins, C.A., and A. DiAntonio. 2007. Synaptic development: insights from *Drosophila*. *Curr. Opin. Neurobiol.* 17:35–42. http://dx.doi.org/10.1016/j.conb.2007.01.001

Collins, C.A., Y.P. Wairkar, S.L. Johnson, and A. DiAntonio. 2006. Highwire restrains synaptic growth by attenuating a MAP kinase signal. *Neuron*. 51:57–69. http://dx.doi.org/10.1016/j.neuron.2006.05.026

DeLotto, Y., and R. DeLotto. 1998. Proteolytic processing of the *Drosophila* Spätzle protein by Easter generates a dimeric NGF-like molecule with ventralising activity. *Mech. Dev.* 72:141–148. http://dx.doi.org/10.1016/S0925-4773(98)00024-0

Featherstone, D.E., and K. Broadie. 2000. Surprises from *Drosophila*: genetic mechanisms of synaptic development and plasticity. *Brain Res. Bull.* 53:501–511. http://dx.doi.org/10.1016/S0361-9230(00)00383-X

Feng, Y., A. Ueda, and C.F. Wu. 2004. A modified minimal hemolymph-like solution, HL3.1, for physiological recordings at the neuromuscular junctions of normal and mutant *Drosophila* larvae. *J. Neurogenet.* 18:377–402. http://dx.doi.org/10.1080/01677060490894522

Ganesan, S., K. Aggarwal, N. Paquette, and N. Silverman. 2011. NF-κB/Rel proteins and the humoral immune responses of *Drosophila* melanogaster. *Curr. Top. Microbiol. Immunol.* 349:25–60.

Govind, S., L. Brennan, and R. Steward. 1993. Homeostatic balance between dorsal and cactus proteins in the *Drosophila* embryo. *Development*. 117:135–148.

Guillemot, F., and C. Zimmer. 2011. From cradle to grave: the multiple roles of fibroblast growth factors in neural development. *Neuron*. 71:574–588. http://dx.doi.org/10.1016/j.neuron.2011.08.002

Hanamsagar, R., M.L. Hanke, and T. Kielian. 2012. Toll-like receptor (TLR) and inflammasome actions in the central nervous system. *Trends Immunol.* 33:333–342. http://dx.doi.org/10.1016/j.it.2012.03.001

Hanke, M.L., and T. Kielian. 2011. Toll-like receptors in health and disease in the brain: mechanisms and therapeutic potential. *Clin. Sci.* 121:367–387. http://dx.doi.org/10.1042/CS20110164

Heckscher, E.S., R.D. Fetter, K.W. Marek, S.D. Albin, and G.W. Davis. 2007. NF-κB, IκB, and IRAK control glutamate receptor density at the *Drosophila* NMJ. *Neuron*. 55:859–873. http://dx.doi.org/10.1016/j.neuron.2007.08.005

Imler, J.L., and L. Zheng. 2004. Biology of Toll receptors: lessons from insects and mammals. *J. Leukoc. Biol.* 75:18–26. http://dx.doi.org/10.1189/jlb.0403160

Jan, L.Y., and Y.N. Jan. 1976. Properties of the larval neuromuscular junction in *Drosophila melanogaster*. *J. Physiol.* 262:189–214.

Jeibmann, A., and W. Paulus. 2009. *Drosophila melanogaster* as a model organism of brain diseases. *Int. J. Mol. Sci.* 10:407–440. http://dx.doi.org/10.3390/ijms10020407

Johnston, M.V. 2004. Clinical disorders of brain plasticity. *Brain Dev.* 26:73–80. http://dx.doi.org/10.1016/S0387-7604(03)00102-5

Kassabov, S.R., Y.B. Choi, K.A. Karl, H.D. Vishwasrao, C.H. Bailey, and E.R. Kandel. 2013. A single Aplysia neurotrophin mediates synaptic facilitation via differentially processed isoforms. *Cell Rep.* 3:1213–1227. http://dx.doi.org/10.1016/j.celrep.2013.03.008

Keshishian, H., K. Broadie, A. Chiba, and M. Bate. 1996. The *Drosophila* neuromuscular junction: a model system for studying synaptic development and function. *Annu. Rev. Neurosci.* 19:545–575. http://dx.doi.org/10.1146/annurev.ne.19.030196.002553

Kittel, R.J., C. Wichmann, T.M. Rasse, W. Fouquet, M. Schmidt, A. Schmid, D.A. Wagh, C. Pawlu, R.R. Kellner, K.I. Willig, et al. 2006. Bruchpilot promotes active zone assembly, Ca^{2+} channel clustering, and vesicle release. *Science*. 312:1051–1054. http://dx.doi.org/10.1126/science.1126308

Kim, S., S. Chung, J. Yoon, K.W. Choi, and J. Yim. 2006. Ectopic expression of Tollo/Toll-8 antagonizes Dpp signaling and induces cell sorting in the *Drosophila* wing. *Genesis*. 44:541–549. http://dx.doi.org/10.1002/dvg.20245

Landgraf, M., T. Bossing, G.M. Technau, and M. Bate. 1997. The origin, location, and projections of the embryonic abdominal motorneurons of *Drosophila*. *J. Neurosci.* 17:9642–9655.

Lee, H., S. Lee, I.H. Cho, and S.J. Lee. 2013. Toll-like receptors: sensor molecules for detecting damage to the nervous system. *Curr. Protein Pept. Sci.* 14:33–42. http://dx.doi.org/10.2174/1389203711314010006

Letiembre, M., W. Hao, Y. Liu, S. Walter, I. Mihaljevic, S. Rivest, T. Hartmann, and K. Fassbender. 2007. Innate immune receptor expression in normal brain aging. *Neuroscience*. 146:248–254. http://dx.doi.org/10.1016/j.neuroscience.2007.01.004

Ma, Y., R.L. Haynes, R.L. Sidman, and T. Vartanian. 2007. TLR8: an innate immune receptor in brain, neurons and axons. *Cell Cycle*. 6:2859–2868. http://dx.doi.org/10.4161/cc.6.23.5018

Mamidipudi, V., X. Li, and M.W. Wooten. 2002. Identification of IRAK as a conserved component in the p75-neurotrophin receptor activation of NF-κB. *J. Biol. Chem.* 277:28010–28018. http://dx.doi.org/10.1074/jbc.M109730200

Marqués, G. 2005. Morphogens and synaptogenesis in *Drosophila*. *J. Neurobiol.* 64:417–434. http://dx.doi.org/10.1002/neu.20165

Marrus, S.B., and A. DiAntonio. 2004. Preferential localization of glutamate receptors opposite sites of high presynaptic release. *Curr. Biol.* 14:924–931. http://dx.doi.org/10.1016/j.cub.2004.05.047

Marrus, S.B., S.L. Portman, M.J. Allen, K.G. Moffat, and A. DiAntonio. 2004. Differential localization of glutamate receptor subunits at the *Drosophila* neuromuscular junction. *J. Neurosci.* 24:1406–1415. http://dx.doi.org/10.1523/JNEUROSCI.1575-03.2004

Martín-Blanco, E., A. Gampel, J. Ring, K. Virdee, N. Kirov, A.M. Tolkovsky, and A. Martinez-Arias. 1998. puckered encodes a phosphatase that mediates a feedback loop regulating JNK activity during dorsal closure in *Drosophila*. *Genes Dev.* 12:557–570. http://dx.doi.org/10.1101/gad.12.4.557

McCabe, B.D., G. Marqués, A.P. Haghighi, R.D. Fetter, M.L. Crotty, T.E. Haerry, C.S. Goodman, and M.B. O'Connor. 2003. The BMP homolog Gbb provides a retrograde signal that regulates synaptic growth at the *Drosophila* neuromuscular junction. *Neuron*. 39:241–254. http://dx.doi.org/10.1016/S0896-6273(03)00426-4

McIlroy, G., I. Foldi, J. Aurikko, J.S. Wentzell, M.A. Lim, J.C. Fenton, N.J. Gay, and A. Hidalgo. 2013. Toll-6 and Toll-7 function as neurotrophin receptors in the *Drosophila melanogaster* CNS. *Nat. Neurosci.* 16:1248–1256. http://dx.doi.org/10.1038/nn.3474

McLachlan, E.M., and A.R. Martin. 1981. Non-linear summation of end-plate potentials in the frog and mouse. *J. Physiol.* 311:307–324.

Minakhina, S., and R. Steward. 2006. Nuclear factor-kappa B pathways in *Drosophila*. *Oncogene*. 25:6749–6757. http://dx.doi.org/10.1038/sj.onc.1209940

Mizutani, C.M., and E. Bier. 2008. EvoD/Vo: the origins of BMP signalling in the neuroectoderm. *Nat. Rev. Genet.* 9:663–677. http://dx.doi.org/10.1038/nrg2417

Mosca, T.J., and T.L. Schwarz. 2010a. *Drosophila* Importin-α2 is involved in synapse, axon and muscle development. *PLoS ONE*. 5:e15223. http://dx.doi.org/10.1371/journal.pone.0015223

Mosca, T.J., and T.L. Schwarz. 2010b. The nuclear import of Frizzled2-C by Importins-β11 and α2 promotes postsynaptic development. *Nat. Neurosci.* 13:935–943. http://dx.doi.org/10.1038/nn.2593

Okun, E., K.J. Griffioen, and M.P. Mattson. 2011. Toll-like receptor signaling in neural plasticity and disease. *Trends Neurosci.* 34:269–281. http://dx.doi.org/10.1016/j.tins.2011.02.005

O'Neill, L.A., and C. Greene. 1998. Signal transduction pathways activated by the IL-1 receptor family: ancient signaling machinery in mammals, insects, and plants. *J. Leukoc. Biol.* 63:650–657.

Packard, M., E.S. Koo, M. Gorczyca, J. Sharpe, S. Cumberledge, and V. Budnik. 2002. The *Drosophila* Wnt, Wingless, provides an essential signal for pre- and postsynaptic differentiation. *Cell*. 111:319–330. http://dx.doi.org/10.1016/S0092-8674(02)01047-4

Packard, M., D. Mathew, and V. Budnik. 2003. FASt remodeling of synapses in *Drosophila*. *Curr. Opin. Neurobiol.* 13:527–534. http://dx.doi.org/10.1016/j.conb.2003.09.008

Park, H., and M.M. Poo. 2013. Neurotrophin regulation of neural circuit development and function. *Nat. Rev. Neurosci.* 14:7–23. http://dx.doi.org/10.1038/nrn3379

Parker, J.S., K. Mizuguchi, and N.J. Gay. 2001. A family of proteins related to Spätzle, the toll receptor ligand, are encoded in the *Drosophila* genome. *Proteins*. 45:71–80. http://dx.doi.org/10.1002/prot.1125

Peled, E.S., and E.Y. Isacoff. 2011. Optical quantal analysis of synaptic transmission in wild-type and rab3-mutant *Drosophila* motor axons. *Nat. Neurosci.* 14:519–526. http://dx.doi.org/10.1038/nn.2767

Prakash, Y.S., H. Miyata, W.Z. Zhan, and G.C. Sieck. 1999. Inactivity-induced remodeling of neuromuscular junctions in rat diaphragmatic muscle. *Muscle Nerve*. 22:307–319. http://dx.doi.org/10.1002/(SICI)1097-4598(199903)22:3<307::AID-MUS3>3.0.CO;2-M

Qiu, P., P.C. Pan, and S. Govind. 1998. A role for the *Drosophila* Toll/Cactus pathway in larval hematopoiesis. *Development*. 125:1909–1920.

Riesgo-Escovar, J.R., and E. Hafen. 1997. Common and distinct roles of DFos and DJun during *Drosophila* development. *Science*. 278:669–672. http://dx.doi.org/10.1126/science.278.5338.669

Rosso, S.B., and N.C. Inestrosa. 2013. WNT signaling in neuronal maturation and synaptogenesis. *Front. Cell. Neurosci*. 7:103. http://dx.doi.org/10.3389/fncel.2013.00103

Roux, P.P., and P.A. Barker. 2002. Neurotrophin signaling through the p75 neurotrophin receptor. *Prog. Neurobiol.* 67:203–233. http://dx.doi.org/10.1016/S0301-0082(02)00016-3

Ruiz-Cañada, C., and V. Budnik. 2006. Introduction on the use of the *Drosophila* embryonic/larval neuromuscular junction as a model system to study synapse development and function, and a brief summary of pathfinding and target recognition. *Int. Rev. Neurobiol.* 75:1–31. http://dx.doi.org/10.1016/S0074-7742(06)75001-2

Ruse, M., and U.G. Knaus. 2006. New players in TLR-mediated innate immunity: PI3K and small Rho GTPases. *Immunol. Res.* 34:33–48. http://dx.doi.org/10.1385/IR:34:1:33

Salinas, P.C. 2005. Retrograde signalling at the synapse: a role for Wnt proteins. *Biochem. Soc. Trans.* 33:1295–1298. http://dx.doi.org/10.1042/BST20051295

Sanyal, S., D.J. Sandstrom, C.A. Hoeffer, and M. Ramaswami. 2002. AP-1 functions upstream of CREB to control synaptic plasticity in *Drosophila*. *Nature*. 416:870–874. http://dx.doi.org/10.1038/416870a

Sanyal, S., R. Narayanan, C. Consoulas, and M. Ramaswami. 2003. Evidence for cell autonomous AP1 function in regulation of *Drosophila* motorneuron plasticity. *BMC Neurosci.* 4:20. http://dx.doi.org/10.1186/1471-2202-4-20

Seppo, A., P. Matani, M. Sharrow, and M. Tiemeyer. 2003. Induction of neuron-specific glycosylation by Tollo/Toll-8, a *Drosophila* Toll-like receptor expressed in non-neural cells. *Development*. 130:1439–1448. http://dx.doi.org/10.1242/dev.00347

Sigrist, S.J., D.F. Reiff, P.R. Thiel, J.R. Steinert, and C.M. Schuster. 2003. Experience-dependent strengthening of *Drosophila* neuromuscular junctions. *J. Neurosci.* 23:6546–6556.

Stathopoulos, A., and M. Levine. 2002. Dorsal gradient networks in the *Drosophila* embryo. *Dev. Biol.* 246:57–67. http://dx.doi.org/10.1006/dbio.2002.0652

Sutcliffe, B., M.G. Forero, B. Zhu, I.M. Robinson, and A. Hidalgo. 2013. Neuron-type specific functions of DNT1, DNT2 and Spz at the *Drosophila* neuromuscular junction. *PLoS ONE*. 8:e75902. http://dx.doi.org/10.1371/journal.pone.0075902

Takeda, K., T. Kaisho, and S. Akira. 2003. Toll-like receptors. *Annu. Rev. Immunol.* 21:335–376. http://dx.doi.org/10.1146/annurev.immunol.21.120601.141126

Tanga, F.Y., N. Nutile-McMenemy, and J.A. DeLeo. 2005. The CNS role of Toll-like receptor 4 in innate neuroimmunity and painful neuropathy. *Proc. Natl. Acad. Sci. USA*. 102:5856–5861. http://dx.doi.org/10.1073/pnas.0501634102

Torroja, L., M. Packard, M. Gorczyca, K. White, and V. Budnik. 1999. The *Drosophila* β-amyloid precursor protein homolog promotes synapse differentiation at the neuromuscular junction. *J. Neurosci.* 19:7793–7803.

Valanne, S., J.H. Wang, and M. Rämet. 2011. The *Drosophila* Toll signaling pathway. *J. Immunol.* 186:649–656. http://dx.doi.org/10.4049/jimmunol.1002302

Wagh, D.A., T.M. Rasse, E. Asan, A. Hofbauer, I. Schwenkert, H. Durrbeck, S. Buchner, M.C. Dabauvalle, M. Schmidt, G. Qin, et al. 2006. Bruchpilot, a protein with homology to ELKS/CAST, is required for structural integrity and function of synaptic active zones in *Drosophila. Neuron*. 49:833–844. http://dx.doi.org/10.1016/j.neuron.2006.02.008

Yagi, Y., Y. Nishida, and Y.T. Ip. 2010. Functional analysis of Toll-related genes in *Drosophila. Dev. Growth Differ.* 52:771–783. http://dx.doi.org/10.1111/j.1440-169X.2010.01213.x

Zapata, J.M., S. Matsuzawa, A. Godzik, E. Leo, S.A. Wasserman, and J.C. Reed. 2000. The *Drosophila* tumor necrosis factor receptor-associated factor-1 (DTRAF1) interacts with Pelle and regulates NFκB activity. *J. Biol. Chem.* 275:12102–12107. http://dx.doi.org/10.1074/jbc.275.16.12102

Zhang, Y.Q., A.M. Bailey, H.J. Matthies, R.B. Renden, M.A. Smith, S.D. Speese, G.M. Rubin, and K. Broadie. 2001. *Drosophila* fragile X-related gene regulates the MAP1B homolog Futsch to control synaptic structure and function. *Cell*. 107:591–603. http://dx.doi.org/10.1016/S0092-8674(01)00589-X

Zhu, B., J.A. Pennack, P. McQuilton, M.G. Forero, K. Mizuguchi, B. Sutcliffe, C.J. Gu, J.C. Fenton, and A. Hidalgo. 2008. *Drosophila* neurotrophins reveal a common mechanism for nervous system formation. *PLoS Biol.* 6:e284. http://dx.doi.org/10.1371/journal.pbio.0060284